MODELING SPORADIC AMYOTROPHIC LATERAL SCLEROSIS (SALS) IN ZEBRAFISH USING ENVIRONMENTAL STRESSORS

by

Jessica Rebecca Marie Morrice

B.Sc., Simon Fraser University, 2012

A THESIS SUBMITTED IN PARTIAL FULFILLMENT OF

THE REQUIREMENTS FOR THE DEGREE OF

MASTER OF SCIENCE

in

THE FACULTY OF GRADUATE AND POSTDOCTORAL STUDIES

(Interdisciplinary Studies)

THE UNIVERSITY OF BRITISH COLUMBIA

(Vancouver)

August 2017

Abstract

Amyotrophic lateral sclerosis (ALS) is characterized by the progressive degeneration of upper and lower motor neurons. The majority of ALS patients are considered of unknown origin, termed sporadic, and are largely assumed to arise from environmental insults. Despite this, research to date has been heavily focused on genetic models of the disease, which represent 10% of ALS cases. Research has made disappointing progress with elucidating disease initiating mechanisms and therapeutic translation in patients. Sporadic ALS (sALS) models may provide substantially more applicable insight into disease pathogenesis, however there is currently a lack of reliable and effective models. Zebrafish offer promising advantages to investigating ALS, with highly conserved biological processes to humans, including genes implicated in human neurodegenerative diseases. Further, they can be used for high throughput toxicity screening and are optically transparent as embryos to allow for high resolution imaging *in vivo*. Here, we investigate using zebrafish as a model for screening for motor neuron defects and hypothesize that exposure to particular environmental toxins can be used to induce ALS-like hallmarks in a zebrafish model. We find that the zebrafish is an efficient and effective model for screening motor neuron toxicity induced by neurotoxins and Bisphenol A (BPA) exposure has a clear dose-response effect on reduced motor neuron length and branching in embryos at 48 hours post fertilization (hpf). We provide evidence that motor axon length as a valid surrogate marker of motor neuron degeneration by confirming the conventional method of measuring the length from a sagittal view in defective motor axons represents their true length in 3 dimensions, and confirm that reduced motor axon length is associated with increased motor neuron death. Further, BPA exposure results in an ALS-like phenotype with reduced motor function at 24 and 48 hpf, reduced neuromuscular junction integrity and microglia activation in embryos at 48 hpf.

Together, these results show that the zebrafish model is advantageous for screening toxin-induced motor neuron death and can be used as a valid model of sALS. This research can be extended to confirm ALS-associated neurotoxins and provide insight into pathogenic mechanisms of sALS.

Lay Summary

Amyotrophic lateral sclerosis (ALS) is a chronic disease which causes the progressive death of motor neuron cells responsible for motor function. There are two main forms of ALS, sporadic ALS (sALS), which is assumed to be caused by environmental toxins and familial ALS (fALS), which is caused by alterations of a gene. Most of what we currently understand about mechanisms driving ALS are based on animal models of fALS, although most patients have sALS. To better understand the disease, animal models of sALS are needed. Zebrafish offer many compelling experimental advantages, such as having highly conserved biological processes to humans, optically transparency for high resolution imaging of cells and producing hundreds of offspring per week. Here, we show that the zebrafish can be used as a valid and efficient model of investigating sALS and also validate markers to quantify motor neuron death commonly used in the literature.

Preface

All aspects of data collection and analysis were performed by myself. Design of research goals were in collaboration with my supervisors, Drs. Christopher A. Shaw and Cheryl C. Gregory-Evans.

At the time of submission, no publications have arisen from work presented in this dissertation.

All procedures involving animals were approved by the UBC animal care committee under certificate A13-0302 issued to Cheryl Gregory-Evans.

Table of Contents

List of Tables

List of Figures

List of Symbols

α - alpha

μ - micro

β - beta

List of Abbreviations

ALS	−	Amyotrophic lateral sclerosis
sALS	−	sporadic ALS
fALS	−	familial ALS
NMJ	−	Neuromuscular junction
α-BTX	−	α-Bungarotoxin
SC	−	Spinal cord
hpf	−	hours post fertilization
PI	−	Propidium Iodide
PTU	−	N-phenylthiourea
μm	−	Micrometers
μM	−	Micromolar
mSOD1	−	misfolded Cu/Zn Superoxide Dismutase
C9orf72	−	Chromosome 9 open reading frame 72
ALS-PDC	−	ALS-Parkinson Dementia Complex
CRISPR	−	Cluster Regularly Interspaced Short Palinodromic Repeats
CaP	−	Caudal Primary motor neuron
MiP	−	Middle Primary motor neuron
RoP	−	Rostral Primary motor neuron
HCl	−	Hydrogen Chloride
$AlCl_3$	−	Aluminum Chloride
BPA	−	Bisphenol A

TEER	−	Touch Evoked Escape Response
E2	−	Estradiol
GPR30	−	G Protein-coupled estrogen Receptor 30
AR	−	Androgen Receptor
ER	−	Estrogen Receptor
PFA	−	Paraformaldehyde

Acknowledgements

Firstly, I would like to express my sincere gratitude to my supervisors Drs. Christopher A. Shaw and Cheryl Gregory-Evans for their continuous support of my MSc study and research, and for their patience, motivation, guidance, and knowledge. I am grateful for their dedication to my project, and for the stimulating discussions regarding my thesis work and general science.

Besides my supervisors, I would like to thank Dr. Silke Cresswell for her support on my thesis committee.

I would also like to express my utmost appreciation to Xianghong Shan for her continuous mentorship with learning zebrafish handling, protocols and techniques. I'm also grateful for her assistance with maintaining the adult zebrafish lines, trouble shooting and screening embryos for transgenesis. I thank Hani Bagheri for his mentorship with learning zebrafish handling and protocols, Agripina Suarez for her endless support, Michael Kuo for his assistance with the behavioural experiments, Janice Yoo for her support with experiments and Housam Eidi for his constructive feedback on my project. I would also like to thank Ishaq Viringipurampeer for his assistance with protocols and while learning confocal microscopy, Naif Sannan and Xia Wang for their support with experiments.

I am grateful for the financial support of my project from the Luther Allyn Shourds Dean Estate Grant.

Finally, I would like to thank both my wonderful parents Kathleen O'Keefe and Ken Morrice for

their unconditional support and encouragement to pursue my own path, along with the rest of my family including Michael Reed, and my friends for their support.

Chapter 1: Introduction

1.1 Amyotrophic Lateral Sclerosis

Amyotrophic lateral sclerosis (ALS) was first described in the late 1800's and is characterized by the progressive degeneration of both upper and lower motor neurons (1). ALS is the most common motor neuron disease with an annual incidence of 2-3 per 100,000 in North America and Europe (2, 3). The average age of symptom onset is between 55-65 and predominantly affects men with a 1.5:1 ratio to women (3). ALS is differentially diagnosed based on clinical evaluation of progressive upper and lower motor neuron defects and exclusion of ALS mimic diseases, such as different myopathies or neuropathies (3). The diagnostic process takes around 12 months due to the lack of a reliable biomarker (3). Most patients present with focal symptom onset in their extremities or bulbar symptom onset which progresses to affect different regions within the body although there is phenotypic variability between patients (3, 4). Patients typically die from asphyxiation within 3 – 5 years of diagnosis (5), although there is considerable heterogeneity in patient survival (3). Despite arduous efforts, research has yet to develop a cure or an effective therapeutic due to largely uncharacterized disease mechanisms (6, 7). Further, research has been unable to provide significant insight into the heterogeneity in disease pathology between patients, such as site on symptom onset, degree multisystem involvement, and disease progression (3). For the past two decades there was only one FDA-approved drug available to patients, which extends life by an average of three months (7). Recently a second therapeutic has been approved and will be available to patients in August 2017 (8). Unfortunately, only mild therapeutic effects are expected from this new treatment (9).

1.2 Etiology

There are two main forms of ALS, about 90% of cases are considered sporadic (sALS) which lack evidence of a hereditary genetic component and the remaining 10% of cases are familial ALS (fALS), which are caused by different genetic mutations (10). Over 25 different genetic mutations have been linked to ALS (11). A hexanucleotide repeat expansion in chromosome 9 open reading frame 72 (*C9orf72)* is currently the most common mutation in fALS, accounting for around 40% of fALS patients (10, 12). The vast majority of investigative and therapeutic research has been based on mutations that result in misfolded Cu/Zn superoxide dismutase 1 (SOD1) proteins. These mutations account for around 10% of fALS cases and less than 2% of all ALS patients (1, 13). Although sALS and fALS patients have a similar clinical pathology at end state disease (14), it is currently unknown if both forms result from the same pathogenic mechanism, and further how relevant research based on genetic models is to sALS pathogenesis (15).

1.3 Environmental Factors Associated With ALS

Evidence from epidemiological studies suggest that environmental factors are associated with sALS etiology (16-20). ALS "clusters", or spatial clustering of increased disease incidence have been identified, such as with the native Chamorro population of Guam (20-22) and in the Kii Peninsula of Japan (23). Both of these clusters show increased incidence of a form of ALS with progressive dementia and parkinsonian features, called ALS-PDC (20). Increased incidence of ALS has also been found in military personnel (24), soccer (25) and football players (26). These groups suggest ALS environmental risk factors, such as military enrolment (24), pesticide (27) and heavy metal exposure (28), diet (18, 29) and high level sports (25, 26). Despite evidence for

various environmental factors having a role in etiology, a causal relationship has yet to be established. Further, a common mechanism between these various environmental factors that may be triggering motor neuron degeneration is not understood.

1.4 Zebrafish as a Model of Neurodegeneration

Zebrafish are emerging as an important and useful vertebrate model for neurodegeneration and offer unique advantages to mammal models (30). Each mating pair can produce around 200 embryos per week (31) or 10,000 embryos per annum (32) and embryos rapidly develop *ex vivo,* which allows for direct *in vivo* observation (31). Zebrafish have a similar, yet simplified nervous system compared to humans (30, 33, 34). The zebrafish genome has been fully sequenced (34), and genes implicated in neurodegenerative diseases are highly conserved. Zebrafish are easily genetically manipulated using different techniques, and have been used extensively for knockdown studies using antisense oligonucleotide morpholinos, knockout studies using cluster regularly interspaced short palinodromic repeats (CRISPR)-Cas9 technology, knock-in studies using transgenesis and further, numerous transgenic models are available with fluorescent reporter genes (30, 35). Further, zebrafish are optically transparent as embryos which allows for high resolution whole mount imaging *in vivo*.

1.4.1 Zebrafish as a Model of ALS

Zebrafish offer unique advantages for modeling motor neuron diseases such as ALS such as a convenient method for estimating motor neuron degeneration. The motor system rapidly develops in embryos which can be directly observed *in vivo,* and embryos have simple stereotypical motor behaviour which is useful for investigating an affected motor function (36).

At 18 hours post fertilization (hpf), primary motor neurons start to exit the ventral root of the spinal cord. By 48 hpf each somite has one set of caudal (CaP), middle (MiP) and rostral (RoP) primary motor neurons innervating each side of the spinal segment (37). Each primary motor neuron innervates specific regions on muscle fibers (37). RoP motor neurons innervate the middle area of muscle fibers, MiP motor neurons innervate dorsal axial muscles and CaP motor neurons innervate ventral axial muscles (38). The CaP motor neurons are most commonly used to quantify motor neuron degeneration in zebrafish studies of ALS (39-42) as they have the most prominent axonal projection and a relatively large soma (38) (Figure 4.1). Conventionally, motor neuron degeneration in zebrafish is estimated by quantifying CaP motor axon length (39-42), although we note that this rarely validated in the literature as a surrogate marker of motor cell death.

Despite the many advantages of modeling ALS in zebrafish, there are important disadvantages to consider. The zebrafish is not a mammal, and also does not have corticospinal or comparable rubricospinal tracts, therefore cannot be used to model upper motor neuron defects.

1.5 Objective and Hypothesis

The pathogenesis of sALS remains largely uncharacterized. ALS research has been heavily weighted on investigating disease pathogenesis using genetic models of the disease, although the vast majority of ALS cases are considered sporadic with no evidence of a heritable genetic component and are assumed to be associated with environmental stressors or toxins. It is currently unknown whether sALS and fALS follow a similar disease pathogenesis, therefore findings based on fALS models may have limited implications for patients. Effective and

validated sporadic ALS models are needed in the field to investigate pathogenesis, therefore the overall objective of my thesis project aims to use zebrafish as a relevant model to characterize an ALS-like phenotype induced by environmental neurotoxins. Here, we investigate using zebrafish as an efficient and effective model for screening for motor neuron abnormalities as a marker for motor neuron degeneration. We hypothesize that exposure to environmental toxins induces an ALS-like phenotype in a zebrafish model, such as reduced motor behaviour, impaired neuromuscular junction integrity and activated microglia.

Chapter 2: Screening Environmental Stressors for an Affected Motor Neuron Phenotype

2.1 Introduction

Zebrafish offer many advantages as compared to mammals for toxin screening studies. Zebrafish can be used for high throughput studies, are less costly to maintain, require shorter exposure time and reduced amount of screening compound (34). Further, zebrafish are a well accepted and an established model for toxicity studies as most environmental pollutants and toxins have been screened for toxicity in zebrafish embryos (34). Here, our main aim is to determine if the zebrafish is an efficient and effective model for screening for neurotoxicity following exposure to candidate environmental stressors.

2.2 Materials and Methods

2.2.1 Fish Husbandry and Lines

Zebrafish (*Danio rerio*) were bred and maintained according to standard procedures (43). All experiments listed were performed within the guidelines of the Canadian Council for Animal Care (CCAC) and the Animal Care Committee of the University of British Columbia. In this chapter, we use the wild type AB zebrafish strain for all experiments listed. Embryos were raised at 28.5°C on a 14 h light/10 h dark cycle in 100 mm^2 petri dishes containing aquaria water. To inhibit pigment formation in embryos and produce clear images using confocal microscopy, 0.003% phenylthiourea (PTU) (v/v) was added to the embryo media at 10 hpf. Unless otherwise stated, all experimental conditions grew ~100 embryos per 50 mL petri dish until neurotoxin exposure and embryo media was changed once per day. Embryos were sacrificed by over-anaesthetizing in 0.1% tricaine (v/v) dissolved in E3 embryo media (5mM NaCl, 0.17mM KCl,

0.33mM $CaCl_2$, 0.33mM $MgCl_2$, 1% methylene blue (v/v)) until the heartbeat was no longer evident.

2.2.2 Neurotoxin Exposure to Zebrafish Embryos

We have looked at various toxic compounds putatively implicated in motor neuron degeneration in zebrafish. Due to this, we have screened some of these candidates for use in our model system. These are ketamine, aluminum chloride and Bisphenol A (BPA). Embryos were staged at 5 hpf and only those with normal morphology were selected for analysis. Embryos were exposed to neurotoxins suspended in E3 embryo media. Approximately 12 embryos per well were placed in a 6 well plate with 5mL treatment or control media. Dead embryos were removed at least once per day.

2.2.3 Ketamine Exposure

Starting at 10 hpf, wild type AB embryos were transferred to E3 media plus 0.003% PTU (v/v) to inhibit pigment development. Stock solution of 100 mg/mL ketamine HCl was used to prepare final working concentrations by diluting stock solution in E3 media plus 0.003% PTU (v/v). Embryos were dechorionated using Dumont fine tip forceps under a Nikon SMZ800 dissecting microscope. Treatment was prepared immediately prior to administration at 28 hpf (Table 2.1). Groups treated with control media were administered E3 media plus 0.003% PTU (v/v). At 48 hpf, embryos were sacrificed and fixed in 4% PFA for 3 hours at room temperature and were stored in 1X PBS at 4^{o}C until whole mount immunohistochemical analysis.

2.2.4 Aluminum Chloride ($AlCl_3$) Exposure

Starting at 10 hpf, wild type AB embryos were transferred to E3 media plus 0.003% PTU (v/v) and dechorionated at 24 hpf. Stock solutions of $AlCl_3$ were prepared by dissolving $AlCl_3$ in $_{dd}H_20$ and sonicating the solution for 30 min. Working concentrations were prepared by serial dilution of stock solution in E3 media plus 0.003% PTU (v/v) and the pH was adjusted to 5.8. At 30 hpf, morphologically normal embryos were exposed to various concentrations of $AlCl_3$ (Table 2.1). Groups treated with control media were administered E3 media plus 0.003% PTU (v/v) and pH control media were administered E3 media plus 0.003% PTU (v/v) with pH adjusted to 5.8. At 48 hpf, embryos were over-anaesthetized and fixed in 4% PFA for 3 hours at room temperature and were stored in 1X PBS at 4^oC until whole mount immunohistochemical analysis.

2.2.5 Bisphenol A (BPA) Exposure

Stock solution of 10 mg/mL BPA was prepared by dissolving BPA granules in 100% DMSO using a vortex. Aliquots were stored at -20^oC and replaced every 6 months with freshly prepared stock solution. Final working solutions were prepared by dissolving 10 mg/mL stock solution with E3 media, with a maximum final volume of 1% DMSO (v/v).

At 6 hpf, embryos were dechorionated by agitated exposure to 1 mg/mL pronase solution for 3.5 minutes, washed 3X in fresh E3 media. Embryos were then immediately exposed to various concentrations of BPA. Groups treated with vehicle control media were administered 1% DMSO (v/v) dissolved in E3 media. Groups treated with control media were administered E3 media alone. Fresh treatment and control media was prepared daily immediately prior to being administered to embryos. To reduce any confounding toxicity effect of static exposure, freshly

prepared treatment was administered once per day until sacrifice. To inhibit pigment formation in embryos and produce clear images using confocal microscopy, BPA treatment was replaced with BPA treatment plus 0.003% PTU (v/v) at 10 hpf (Table 2.1). At 48 hpf, embryos were over-anaesthetized and fixed in 4% PFA for 3 hours at room temperature and were stored in 1X PBS at 4^{o}C until whole mount immunohistochemical analysis.

Table 2.1 Developmental Time Point of Neurotoxin Exposure

Neurotoxin	Developmental time point	Solution
Ketamine	10 hpf	E3 media plus 0.003% PTU
	24 hpf	Replace E3 media plus 0.003% PTU
	28 hpf	1.6 - 4 mM ketamine + E3 media plus 0.003% PTU
$AlCl_3$	10 hpf	E3 media plus 0.003% PTU
	24 hpf	Replace E3 media plus 0.003% PTU
	30 hpf	1 - 100 μg/L $AlCl_3$ + E3 media plus 0.003% PTU
BPA	6 hpf	1 – 50 μM BPA + E3 media
	10 hpf	BPA + E3 media plus 0.006% PTU
	24 hpf	Replace BPA + E3 media plus 0.006% PTU

2.2.6 Whole Mount Immunohistochemistry

For immunolabeling of motor axons, embryos were washed with 0.1% PBS-Tween 20 (v/v) (2 X 10 min). For antigen retrieval, embryos were incubated in 150 mM Tris HCl pH 9 for 5 minutes at room temperature, then 15 minutes at 70^{o}C. Embryos were then washed with 0.1% PBS-

Tween 20 (2 X 5 min) and washed with distilled water (1 X 5min). As a final step in antigen retrieval, embryos were incubated in acetone at -20^{o}C for 15 minutes. Embryos were washed in 0.1% PBS-Tween 20 (3 X 1min) and transferred to a 24 well plate. Embryos were incubated in blocking buffer for 1 hour at room temperature, followed by overnight incubation at 4^{o}C with primary antibody znp-1 (1:200) to label motor axons. The primary antibody was washed off with 0.8% PBS-Triton X-100 (2 X 30min), then washed with PBS-TS (1% Triton, 10% normal goat serum, 1X PBS (v/v)) at room temperature (3 X 30 min). Embryos were then incubated in secondary antibody FITC goat anti-mouse (1:500 dilution in incubation buffer: 1% normal goat serum, 0.8% Triton X-100, 1% BSA, 0.1% PBS-Tween 20 (v/v)) for 2h at room temperature. Embryos were then washed with PBS-TS (2 X 1hr) and stored in 1X PBS at 4^{o}C until flat mounting. All washes and incubations were preformed on a rocking plate at room temperature unless otherwise stated.

2.2.7 Flat Mounting

Yolk sac micro dissection of 48hpf embryos was performed using Dumont fine tip forceps under a Nikon SMZ800 dissecting microscope. Embryos were washed in 1X PBS and oriented sagittally on a round coverslip in Vectashield anti-fade mounting media. Coverslips were then placed on a Fisherbrand Superfrost Plus Microscope slide and the edges were glued using DPX mountant and allowed to dry at least one hour prior to imaging.

2.2.8 Image Acquisition and Analysis of Motor Axon Length

Following flat mounting, motor neurons were and imaged in sagittal Z-stack sections by confocal microscopy. All images were captured within the 6-10 somite region using 20x objective lens by

a Zeiss LSM 510 laser scanning confocal microscope. Maximum projection images were reconstructed from Z-stack images using the Zen 2009 software. After setting a scale bar, maximum projection images were exported as TIFF files and analyzed using the ImageJ software. First, the scale bar was calibrated in ImageJ, then the freehand trace tool was used to measure the distance where the CaP motor axons extended from the spinal cord to the most ventral axonal projection. The mean length of 5 axons per embryo (5 technical replicates) was recorded and the mean of each treatment group (biological replicates) was reported ±SD.

2.3 Results

Screening for reduced motor axon length was used as a surrogate marker for motor axon degeneration following neurotoxin exposure in zebrafish embryos.

2.3.1 Ketamine-Induced Motor Neuron Abnormalities

Wild type embryos were screened for reduced motor axon length following exposure to 0, 1.6, 2.0, 2.5 and 4.0 mM ketamine. Exposure doses were based on findings published by (44). At 48 hpf, embryos were fixed and whole mount immunohistochemistry was performed to label motor neurons. Embryos treated with 2.0 mM ketamine have a statistically significant reduced motor axon length at 48 hpf (Figure 2.1, $P = 0.04$, Mann Whitney U-test). There was no statistical significant difference in axon length in a lower exposure dose of 1.6 mM or 2.5 and 4.0 mM ketamine. However, higher exposure doses show a slight trend in increased axon length. This suggests that another pathway is being activated which interferes with the phenotype of interest. These results indicate that ketamine does not produce a clear dose-response effect on motor axon

abnormalities. Motor axon length per sample represents the average of 4 - 5 CaP motor axons within the 6 - 10 somite region with N = 5 biological replicates.

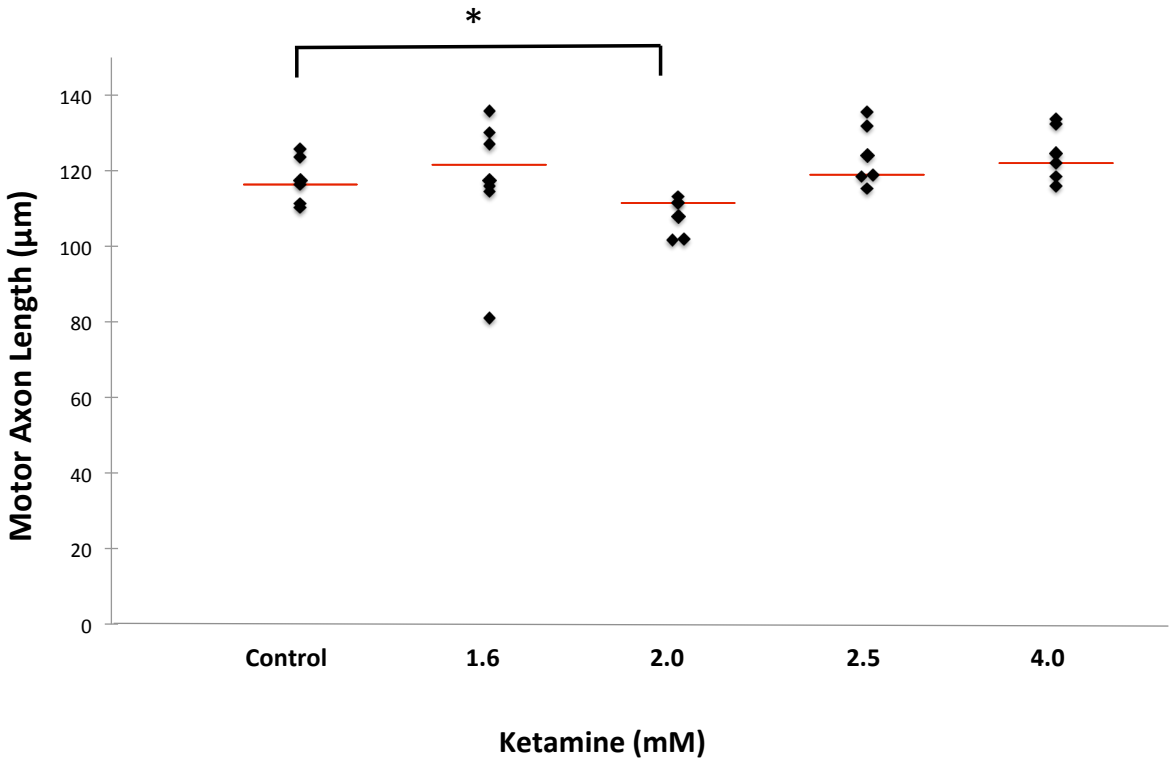

Figure 2.1 Motor Axon Length Following Ketamine Exposure. Wild type embryos were exposed to static treatment of control or ketamine at 28 hpf. Analysis of label motor axons was performed at 48 hpf by whole mount immunohistochemistry. 2.0 mM ketamine exposure results in significantly decreased length (P = 0.04, N= 5) of motor axons. Exposure to 1.6 mM, 2.5 mM and 4.0 mM ketamine results in no significant difference in motor axon length.

2.3.2 Aluminum Chloride ($AlCl_3$)-Induced Motor Neuron Abnormalities

Embryos were screened for reduced motor axon length following 24 hour exposure to $AlCl_3$. Aluminum exposure doses were based on findings from (45) as producing motor behaviour defects in adult zebrafish. Wild type embryos exposed to 1, 10, 50 or 100 µg/L $AlCl_3$ were fixed at 48 hpf and motor axons were labeled using whole mount immunohistochemistry. $AlCl_3$ exposure did not produce a significant difference in axon length (Figure 2.2, N = 2 - 5). Based on

previous groups findings that $AlCl_3$ results in motor defects in older zebrafish, these negative results may be interpreted that aluminum is toxic to motor neurons at a longer duration of exposure, higher doses or exposure may only be toxic at particular developmental periods in zebrafish. Motor axon length per sample represents the average of 4 - 5 CaP motor axons within the 6 - 10 somite region with N = 2 - 5 biological replicates.

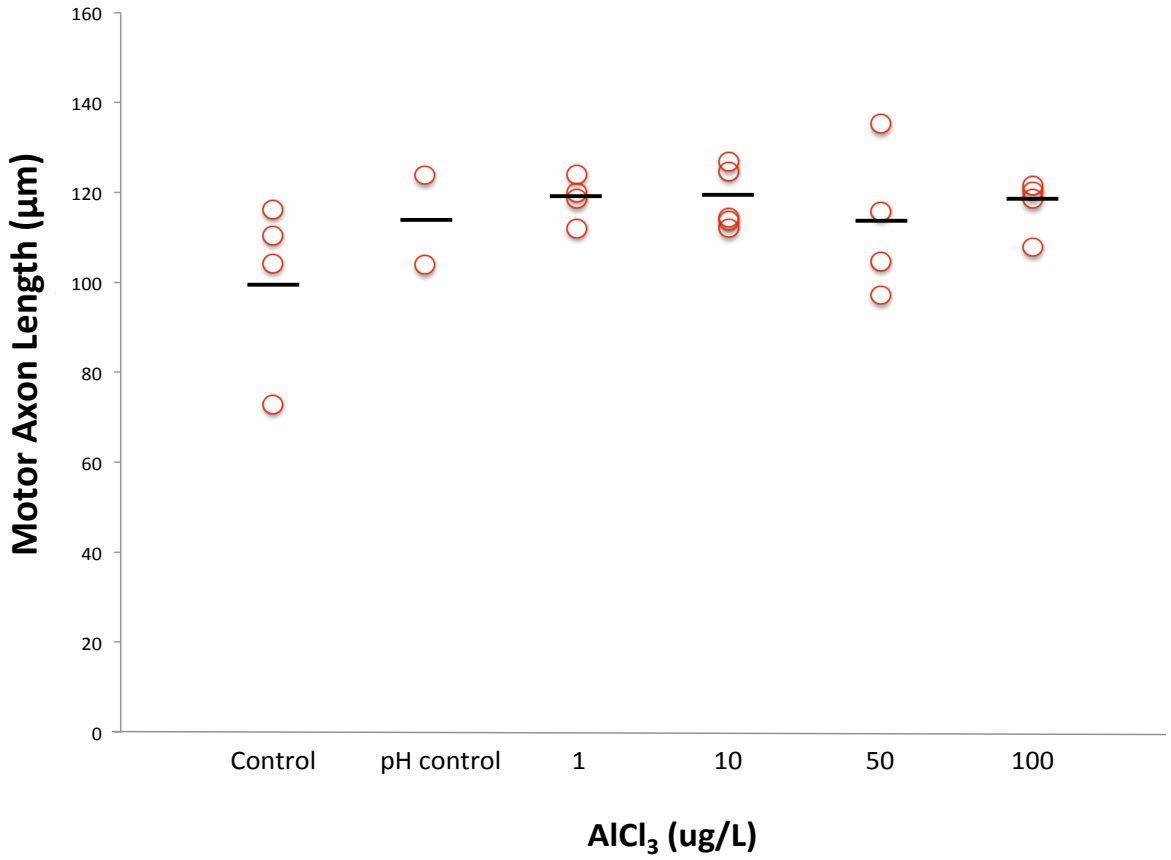

Figure 2.2 Motor Axon Length Following Exposure to $AlCl_3$. Wild type embryos were exposed to static treatment of control, pH control or $AlCl_3$ at 24 hpf and analyzed at 48 hpf by whole mount immunohistochemistry using znp-1 primary antibody to label motor axons. None of the $AlCl_3$ exposure doses had an effect on reduced motor axon length (N = 2 – 5).

2.3.3 Bisphenol A (BPA)-Induced Motor Neuron Abnormalities

Wild type embryos were screened for reduced motor axon length following 42 hours of chronic non-static exposure to 1, 5, 15 and 50 µM BPA, based on the protocol by (46). At 48 hpf,

embryos were fixed and motor axons were labeled using whole mount immunohistochemistry. Results show that the highest dose tested of 50 µM BPA results in significantly shorter motor axon length (Figure 2.3, P <0.0001, Mann-Whitney U test). Motor axon length per sample represents the average of 4 - 5 CaP motor axons within the 6 - 10 somite region with N = 7 – 10 biological replicates. This method of neurotoxin exposure was carried forward for further analysis of BPA-induced motor neuron toxicity.

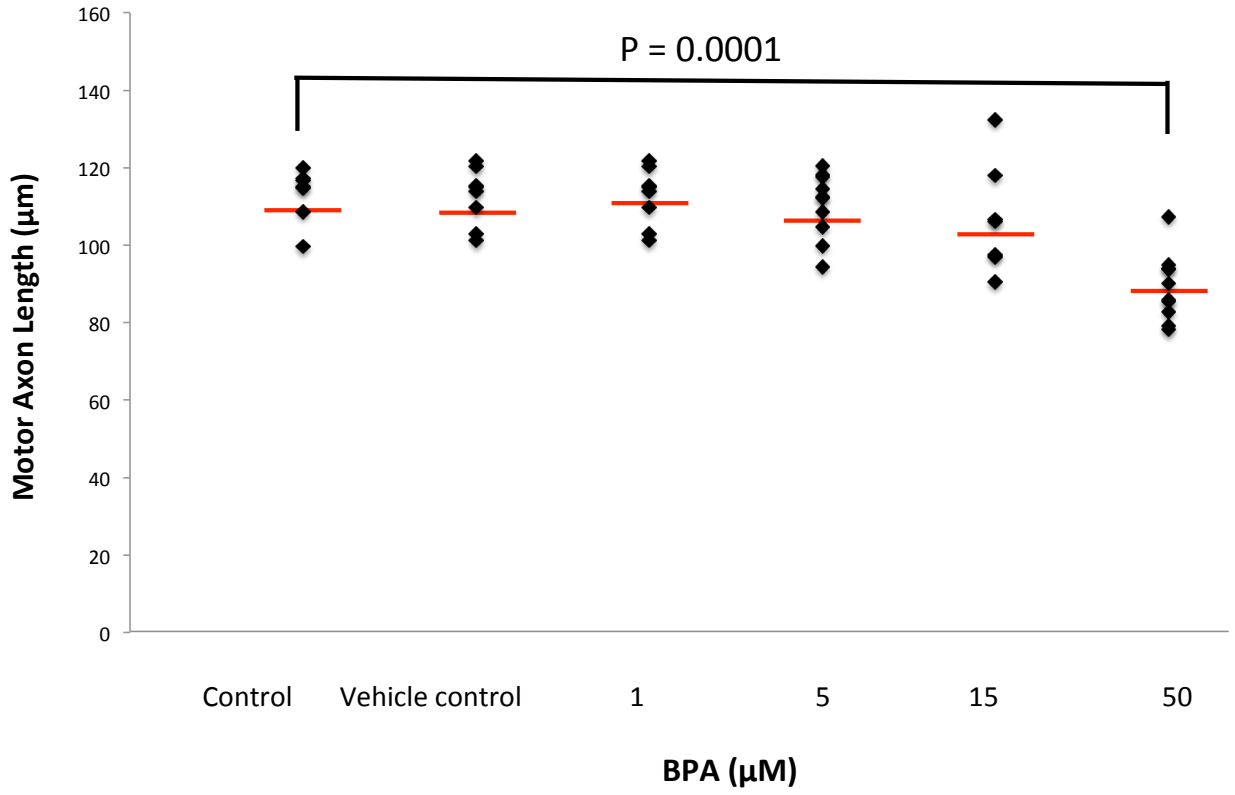

Figure 2.3 Motor Axon Length Following Exposure to BPA. Wild type embryos were exposed to chronic non-static treatment of control, vehicle control or BPA at 6 hpf and analyzed at 48 hpf by whole mount immunohistochemistry using znp-1 primary antibody to label motor axons. Results show that 50 µM BPA treatment results in significantly shorter motor axon length (P < 0.0001; N = 7-10).

Of the compounds tested for motor neuron defects, only BPA produced significantly reduced axon length and for this reason we chose to pursue more detailed parametric studies using this compound.

Chapter 3: Characterizing BPA Induced Motor Axon Defects

3.1 Introduction

For the purpose of further describing the effect of this environmental stressor on neurotoxicity, the effect of BPA exposure on motor axon defects including embryonic lethality was investigated. The duration of exposure and neurodevelopmental effects of BPA were also investigated. Toxicity studies commonly use dose-dependent relationships to understand the relationship between an exposure and the resulting phenotype (47). Zebrafish models of ALS conventionally use motor axon length and branching as markers of neurodegeneration (39-42), therefore to determine if BPA exposure has a clear relationship with motor neuron toxicity, a range of concentrations were tested to determine if non-lethal doses of BPA produce dose-dependent effect on motor axon length and branching.

3.2 Materials and Methods

3.2.1 Zebrafish Lines

We used the wild type AB and the transgenic *Tg*:*mnx1-GFP* (48) (ZFIN ID: ZDB-ALT-051025-4) zebrafish strains for all experiments listed. The transgenic *Tg:mnx1-GFP* strain has GFP expression driven by the mnx1 or hb9 promoter, which specifically labels motor neurons (48). The *Tg:mnx1-GFP* line was used for direct imaging of motor axons and soma. Zebrafish maintenance and husbandry was performed as described in section 2.1.1.

3.2.2 Analysis of Motor Axon Branching

Labeling and analysis of motor axon branches was performed by whole mount immunohistochemistry using the znp-1 primary antibody. Image acquisition and Z-stack

reconstruction was performed as stated in section 2.2.8 for motor axon length. To analyze motor axon branching, TIFF files were uploaded into ImageJ and the software scale was calibrated. The mean number of branches >10 μm emerging from the two most rostral motor axons per embryo within the 6 - 10 somite region were recorded and the mean ± SD from each treatment group was reported.

3.2.3 Motor Behaviour

Motor behaviour was tested using Touch Evoked Escape Response (TEER). At 24 hpf and 48 hpf, the tail region was lightly stimulated using blunt forceps and their movement was recorded using a Leica MZ16 F microscope with a Leica IC80 HD video recording camera. Embryos were considered to have affected motor function when no movement was observed within 10 seconds following a light tactile stimulation on the tail region.

3.2.4 Statistics

All data was tested for normal distribution using the Shapiro-Wilk test. Parametric data were analyzed using a students t-test, and non-parametric data were analyzed using Kruskal-Wallis ranked sums and Mann-Whitney U tests. Data was considered significant at $P < 0.05$.

3.3 Results

BPA exposure showed evidence of a time-dependent exposure effect and these effects did not depend on neurodevelopmental stage of exposure. BPA has a clear dose-response effect on both motor axon length and branching, reaching significance starting at 50 μM BPA exposure.

3.3.1 Effect of Time-Dependent Exposure of BPA on Neurotoxicity

To determine the duration of exposure effect that BPA has on neurotoxicity, motor axon length was evaluated at 24 hpf. Wild type embryos were exposed to control, vehicle control or BPA at 6 hpf and fixed at 24 hpf and 48 hpf. At 24 hpf, motor axons show a decreased trend in length, although this did not reach significance (Figure 3.1). At 48 hpf, 50 μM BPA treatment results in significantly shorter motor axon length ($P < 0.0001$, Mann-Whitney U test). Motor axon length per sample represents the average of 4 - 5 CaP motor axons within the 6 - 10 somite region with N = 2 - 5 biological replicates.

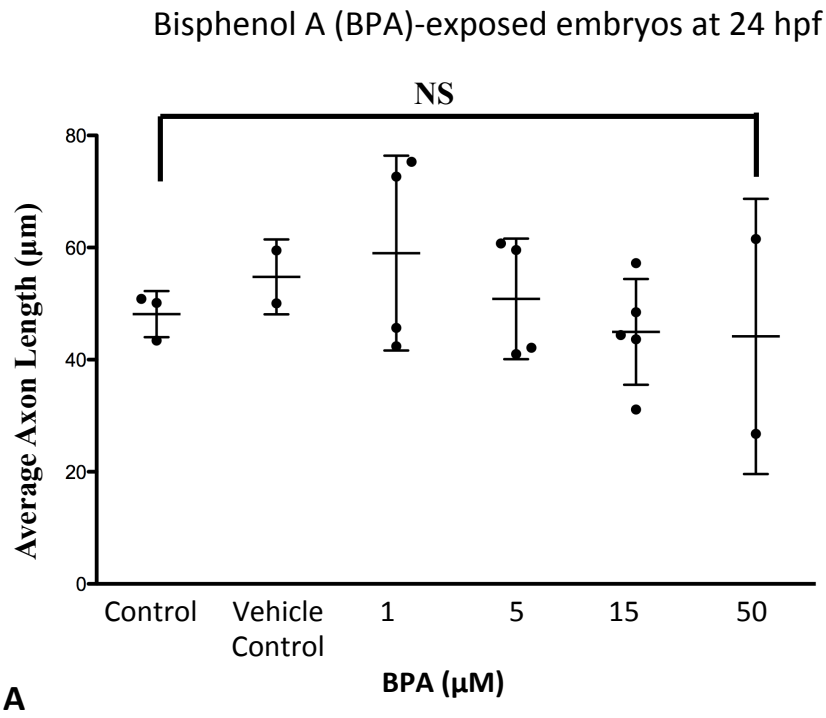

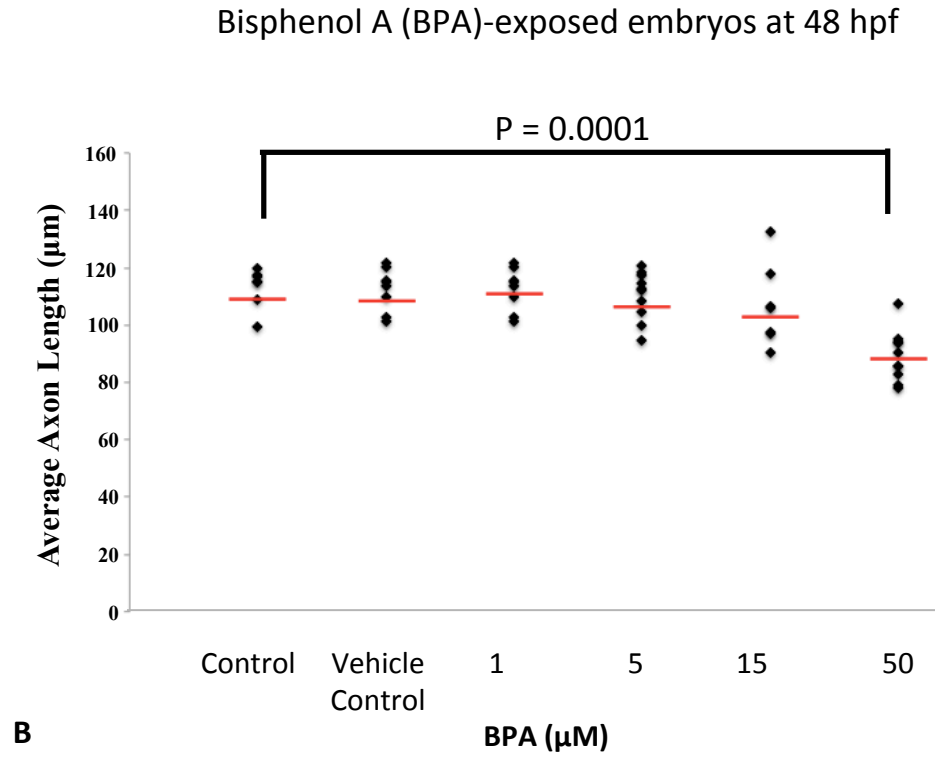

Figure 3.1 Effect of Time-Dependent Exposure of BPA on Neurotoxicity. Wild type embryos were exposed to control, vehicle control or BPA at 6 hpf and fixed at 24 hpf and 48 hpf. A) At 24 hpf, motor axons show a decreased trend in length, although not significant (N= 2 – 5). B) At 48 hpf, 50 µM BPA treatment results in significantly shorter motor axon length (P < 0.0001; N = 7-10).

3.3.2 Neurodevelopmental Exposure of BPA on Adverse Motor Effects

To determine if the neurotoxic effect of BPA is based on the neurodevelopmental time point of exposure, embryos were exposed to BPA at a later time point in development. *Tg:mnx1-GFP* embryos treated with 50 µM BPA at 12 hpf instead of 6 hpf. Mortality and motor function were evaluated at 24 hpf and 48 hpf and embryos were fixed at 48 hpf in 4% PFA. There was no evidence for increased mortality at 24 hpf or 48 hpf following BPA exposure at 12 hpf (Table 3.1). Results show that BPA-exposed embryos had significantly reduced motor axon length (P = 0.04, Mann-Whitney U test, Figure 3.2 A) as compared to vehicle controls. The motor function of BPA exposed embryos showed no evidence of an abnormal escape response at 24 hpf, however 100% of embryos showed evidence of affected motor behaviour at 48 hpf, as indicated by no escape response to a tactile stimulation (Table 3.2). Motor axon length per sample represents the average of 4 – 5 CaP motor axons within the 6 - 10 somite region with N = 8 biological replicates. Mortality and motor function was based on N = 11 biological replicates.

Table 3.1 Embryonic mortality

	24 hpf	48 hpf
Vehicle Control	0%	0%
50 µM BPA	0%	0%

Table 3.2 Embryos with a failed motor response

	24 hpf	48 hpf
Vehicle Control	0%	0%
50 µM BPA	0%	100%

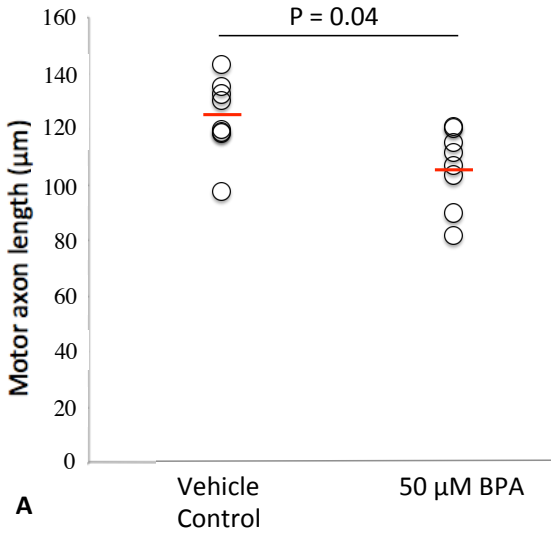

Figure 3.2 Neurodevelopmental Exposure of BPA on Adverse Motor Effects. A) *Tg:mnx1-GFP* embryos treated with 50 µM BPA at 12 hpf (instead of 6 hpf) have significantly (P = 0.04, N = 8) shorter motor axon length at 48 hpf as compared to vehicle controls. The was no evidence of increased mortality (Table 3.1) of BPA exposure at 12 hpf. Embryos exposed to BPA at 12 hpf had a normal escape response at 24 hpf and had a failed motor response at 48 hpf (Table 3.2).

3.3.3 Effect of BPA on Mortality

At 24 hpf, mortality data show that 200 µM BPA results in 100% embryonic lethality. At 48 hpf, data show that 90 µM and 100 µM BPA results in 27% and 100% embryonic lethality, respectively (Table 3.3). 60 µM BPA results in 6.67% mortality at 48 hpf, which was not considered to be substantial when determining the optimal effect-mortality dosage. Teratogenic effects of BPA exposure is listed in Appendix C.

Table 3.3 Lethal Exposure Doses of BPA

	Control	Vehicle control	15 µM BPA	50 µM BPA	60 µM BPA	70 µM BPA	80 µM BPA	90 µM BPA	100 µM BPA	200 µM BPA
24 hpf	0%	0%	0%	0%	0%	0%	0%	0%	0%	100%
48 hpf	0%	0%	0%	0%	6.7%	0%	0%	26.7%	100%	NA

3.3.4 Dose-Response Effect of BPA on Motor Axon Length

The effect of BPA on motor axon length was repeated using higher doses to investigate whether BPA produces a dose-response effect on reduced motor axon length in order to investigate the relationship with motor neuron toxicity. An initial dose-response experiment exposed wild type embryos to 15, 50, 100 and 200 µM BPA. As discussed above in section 3.3.3, 200 µM BPA exposure dose produced 100% mortality by 24 hpf and 100 µM BPA produced 100% mortality by 48 hpf. The remaining samples were fixed at 48 hpf in 4% PFA and motor axons were labeled by whole mount immunohistochemistry. Results (Appendix D) show that exposure to 50 µM BPA results in significantly shorter motor axons ($P = 0.00035$, Mann-Whitney U test, $N = 9$ - 10), confirming findings from the BPA neurotoxicity screen (Figure 2.3). The second attempt to investigate a dose-response effect on motor axon abnormalities tested exposure doses of 15, 50,

60, 70, 80, 90 and 100 µM BPA. Again, 100 µM BPA produced 100% embryonic mortality by 48 hpf. Results show a clear dose-response effect of BPA on motor axon length (Figure 3.3), where exposure to 50, 60, 70, 80 and 90 µM BPA produce statistically significant reduced motor axon length at 48 hpf ($P < 0.0001$, Kruskal-Wallis, Mann-Whitney U post test). Data are based on the mean value of N = 5 - 6 technical replicates and N = 8 - 10 biological replicates.

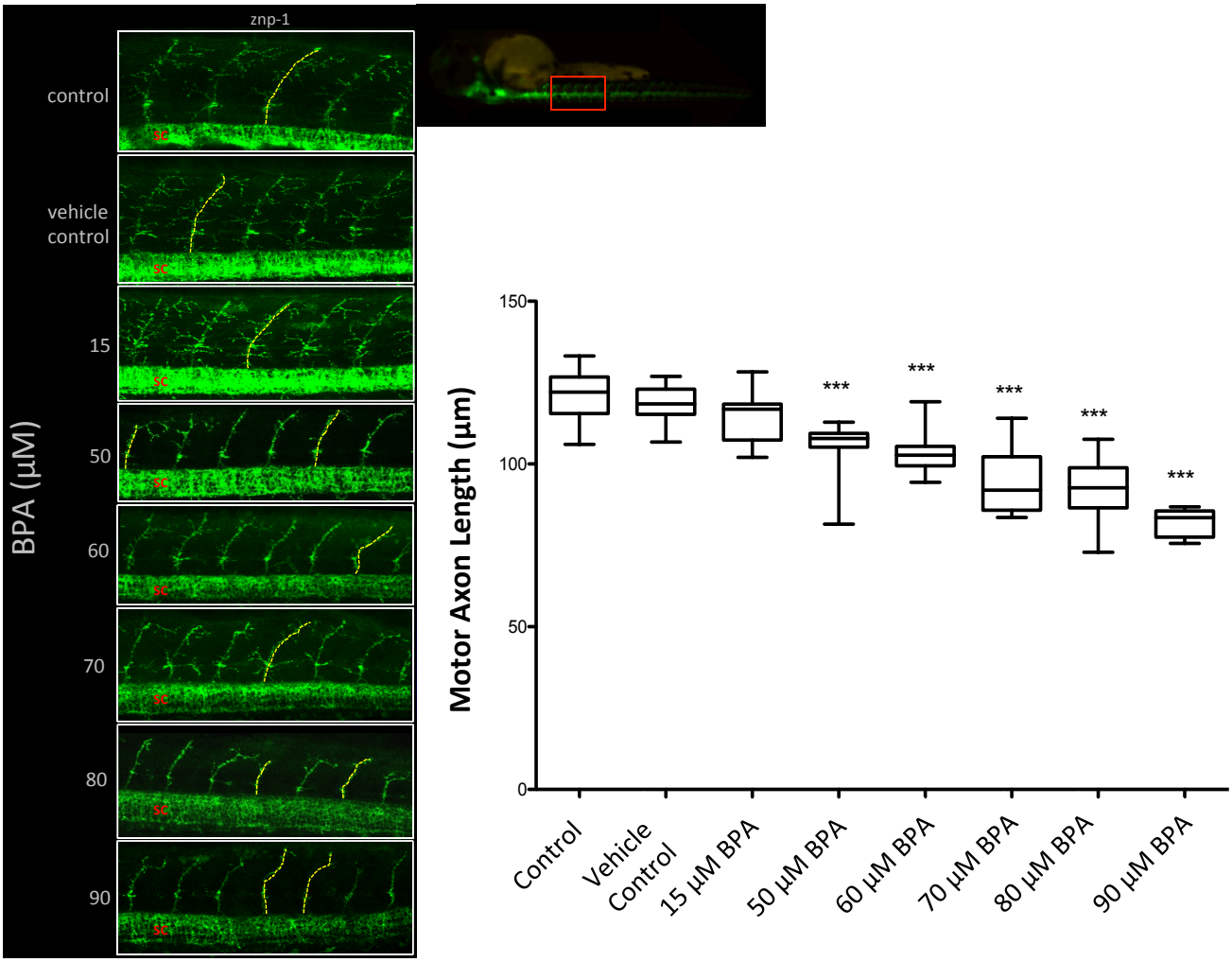

Figure 3.3 Dose-Response Effect of BPA on Motor Axon Length. Wild type embryos exposed to BPA at 6hpf have significantly decreased motor axon length at 50, 60, 70, 80, 90 uM BPA as compared to controls at 48 hpf ($P < 0.0001$; N = 8-10).

3.3.5 Dose-Response Effect of BPA on Motor Axon Branching

The dose-response effect of BPA on motor axons abnormalities was also analyzed for the effect on motor axon branching at 48 hpf. Further analysis of these data show that BPA results in reduced motor axon branching, reaching significance at 50 μM BPA ($P = 0.034$, Mann-Whitney U post test) and dose-response effect (Figure 3.4) at higher doses of 60 – 90 μM BPA ($P < 0.001$, Kruskal-Wallis, Mann-Whitney U post test). Data are based on the mean value of $N = 2$ technical replicates and $N = 8$-10 biological replicates. Further analysis of motor axon defects show that reduced motor axon length is positively correlated to reduced branching (Figure 3.5). From these data, the optimal dose to reduce motor axon length and branching without significant mortality was determined to be 50 μM BPA, which was used for all subsequent analysis described in this thesis.

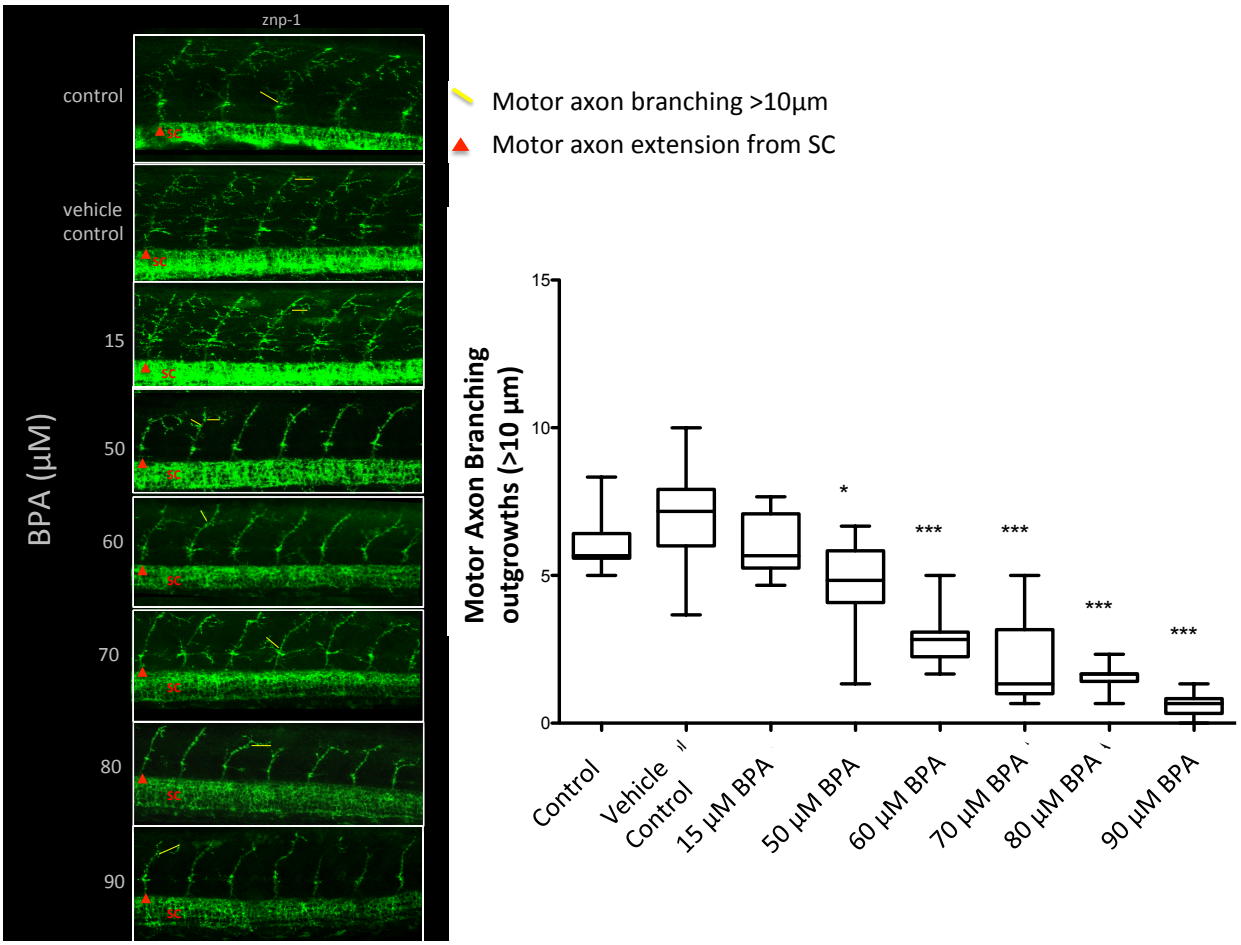

Figure 3.4 Dose-Response of BPA on Motor Axon Branching. Wild type embryos treated with 50, 60, 70, 80, 90 uM BPA at 6hpf have significantly less motor axon branching (>10 um) at 48 hpf. *P = 0.034; ***P < 0.001, Mann-Whitney U test, N = 8 – 10; SC = spinal cord.

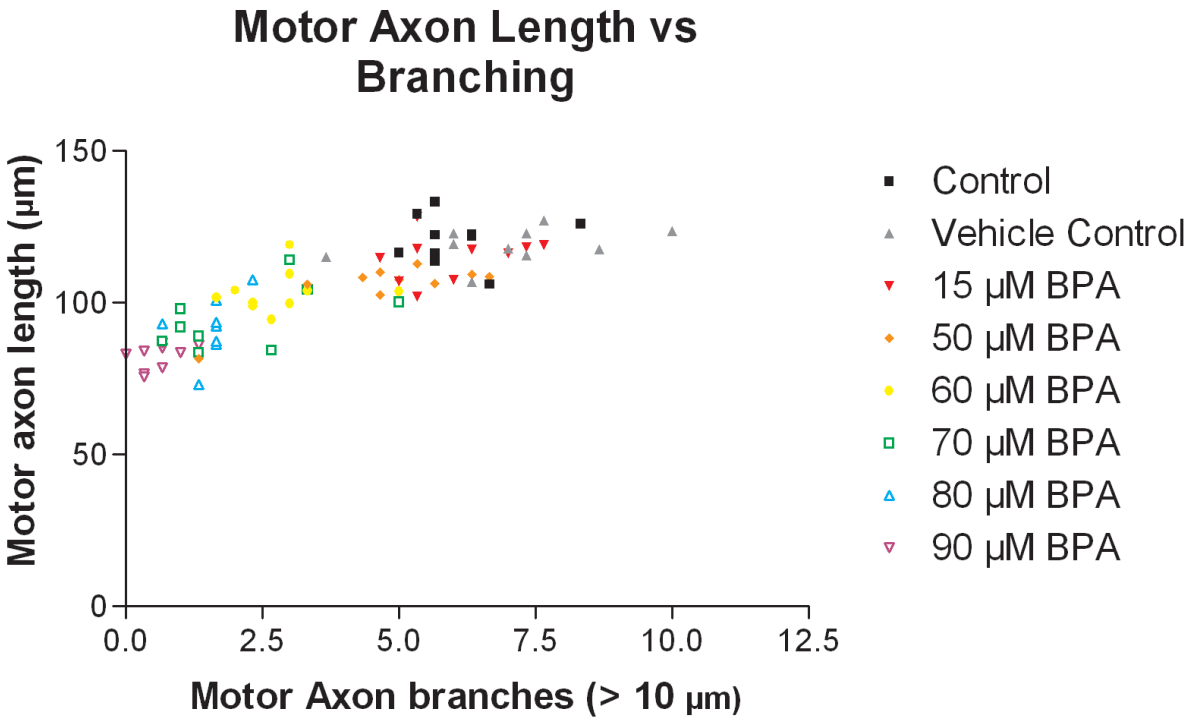

Figure 3.5 Positive Trend Between Motor Axon Length and Branching Defects. Wild type embryos exposed BPA show a positive dose-dependent correlation in motor axon length and branching at 48 hpf (biological N = 8-10), indicating that reduced motor axon length and branching are associated.

Chapter 4: Validating Motor Neuron Length as a Marker for Motor Neuron Degeneration

4.1 Introduction

In zebrafish studies of ALS, the conventional method to estimate motor neuron degeneration in embryos is to analyze the length of the CaP motor neurons at 48 hpf (39-42). Although many groups have used and continue to rely on motor axon length as a surrogate marker for neurodegeneration in zebrafish (39-42), it has yet to be validated in the literature. Our aim was to determine if the 2-dimensional motor axon length from a sagittal plane accurately represents the length of the 3-dimensional trajectory through the Z axis, or if the angle of trajectory is such that a 2-dimensional view would misrepresent the true length (Figure 4.1). Further, studies that show evidence of decreased motor axon length are often unaccompanied with evidence of motor neuron death. As such, we investigated evidence of motor cell death in our model of toxin exposure-induced motor neuron abnormalities.

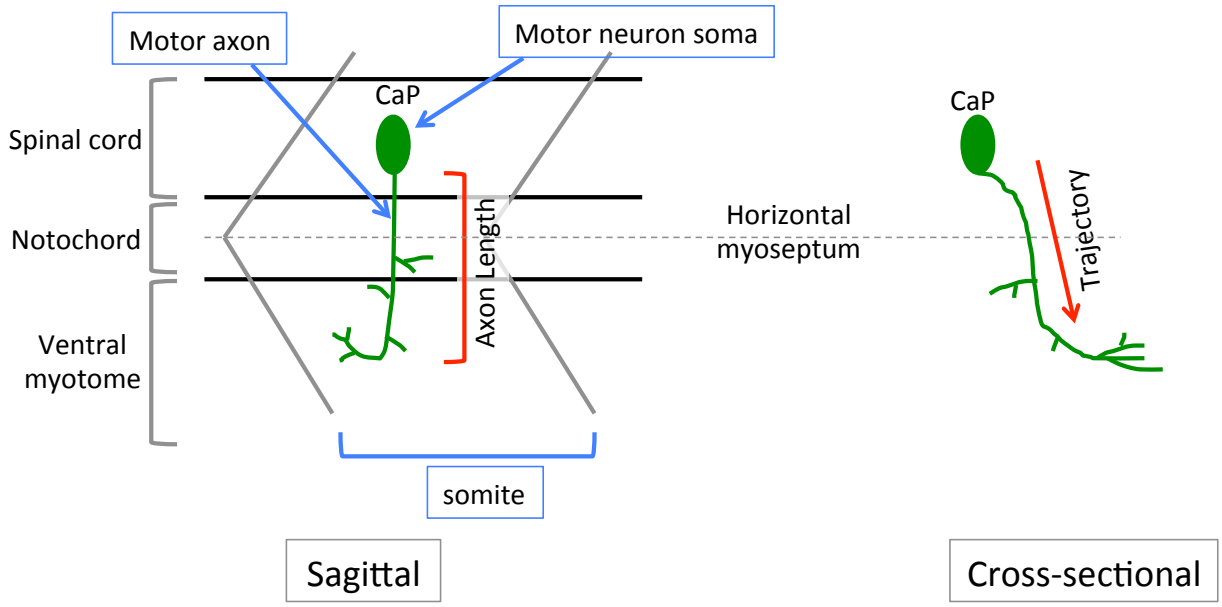

Figure 4.1 Motor Neuron Morphology From a Sagittal and Cross Sectional View. CaP Motor axons project ventrally from the SC to the ventral myotome. Axon length is conventionally measured sagittally, where abnormal motor axons and controls has been assumed to follow the same trajectory.

4.2 Materials and Methods

4.2.1 Morphology of Defective Motor Neurons

Tg:*mnx1-GFP* embryos were exposed to chronic non-static 50 µM BPA starting at 6 hpf and fixed in 4% PFA as detailed in section 2.2.5 at 24 hpf, 48 hpf, 72 hpf and 96 hpf.

4.2.2 Image Microscopy for Motor Neuron Morphology

Embryos were flat mounted as described in section 2.2.7 and imaged using a Zeiss LSM 510 confocal microscope with a 40x water emersion objective lens. Z-stack images of the motor neuron soma in the spinal cord and their projecting axons were collected between the 6 - 10 somite region. High quality and detailed images were collected from *Tg:mnx1-GFP* embryos at 48 hpf by setting the image scanning speed to 7 and averaging of 2.

4.2.3 3-Dimensional Motor Neuron Reconstruction

Lsm files containing Z-stack images were uploaded to NeuronStudio software and reconstructed in the 3-dimensional (3D) viewer. The ZY axis was set to view the motor axon trajectory through the Z plane. Analysis of motor axon trajectory was based on deviation from the Z axis. Trajectory of 3 axons (technical replicates) and 3 embryos per group (biological replicates) were qualitatively analyzed for deviation from the Z axis as compared to vehicle controls.

4.2.4 Time Point Analysis of Motor Neuron Cell Death

As described in section 2.2.5, *Tg:mnx1-GFP* embryos were exposed to chronic, non-static 50 μM BPA or vehicle control and fixed in 4% PFA at 24 hpf, 48 hpf, 72 hpf, 96 hpf and 120 hpf. Analysis of motor neuron cell death was performed by staining with propidium iodide (PI) as a non pathway-specific cell death marker.

4.2.5 Propidium Iodide Staining and Image Acquisition

1 mg/mL stock Propidium Iodide (PI) was diluted to a working concentration of 12 μM in 1X PBS. *Tg:mnx1-GFP* embryos were incubated whole mount in 12 μM PI for 13 min on a rocking plate at room temperature, washed in 1X PBS (3 X 7 min) and stored in 1X PBS at 4^0C until flat mounting and image acquisition. LSM files of Z-stack images of GFP+ motor neuron soma and PI+ cells in the 6 - 10 somite region of the spinal cord were attained by confocal microscopy using a 40x water emersion objective.

4.2.6 Colocalization Analysis: Motor Cell Death

Z-stack LSM files of PI+ cells and motor neuron soma were uploaded to FIJI (a version of ImageJ) and the channels were split. The background was subtracted for each stack in both channels with a rolling ball radius of 50 pixels. The noise was de-speckled for the green channel (motor neuron soma) and a region of interest (ROI) was carefully placed to encompass motor neuron soma in the spinal cord. Colocalization analysis was performed for each Z-stack using the Coloc 2 plugin, and Costes threshold was applied. Manders M2 colocalization coefficient was reported for both vehicle control and 50 μM BPA treated samples. Cells were considered as dead motor neurons by Manders M2 colocalization coefficient of PI+/GFP+ cells in the spinal cord.

4.3 Results

Using this model of environmentally-induced motor neuron abnormalities, our results support measuring 2-dimensional CaP motor axon length at 48 hpf is a valid marker of 3D length and provide preliminary evidence that motor neurons are undergoing cell death.

4.3.1 Motor Axon Trajectory

Tg:mnx1-GFP embryos treated with 50 μM BPA or vehicle control had a similar Z axis trajectory (Figure 4.2). This qualifies using a 2-dimensional sagittal view of motor axons as a valid method of estimating the length of the true 3D axon trajectory length.

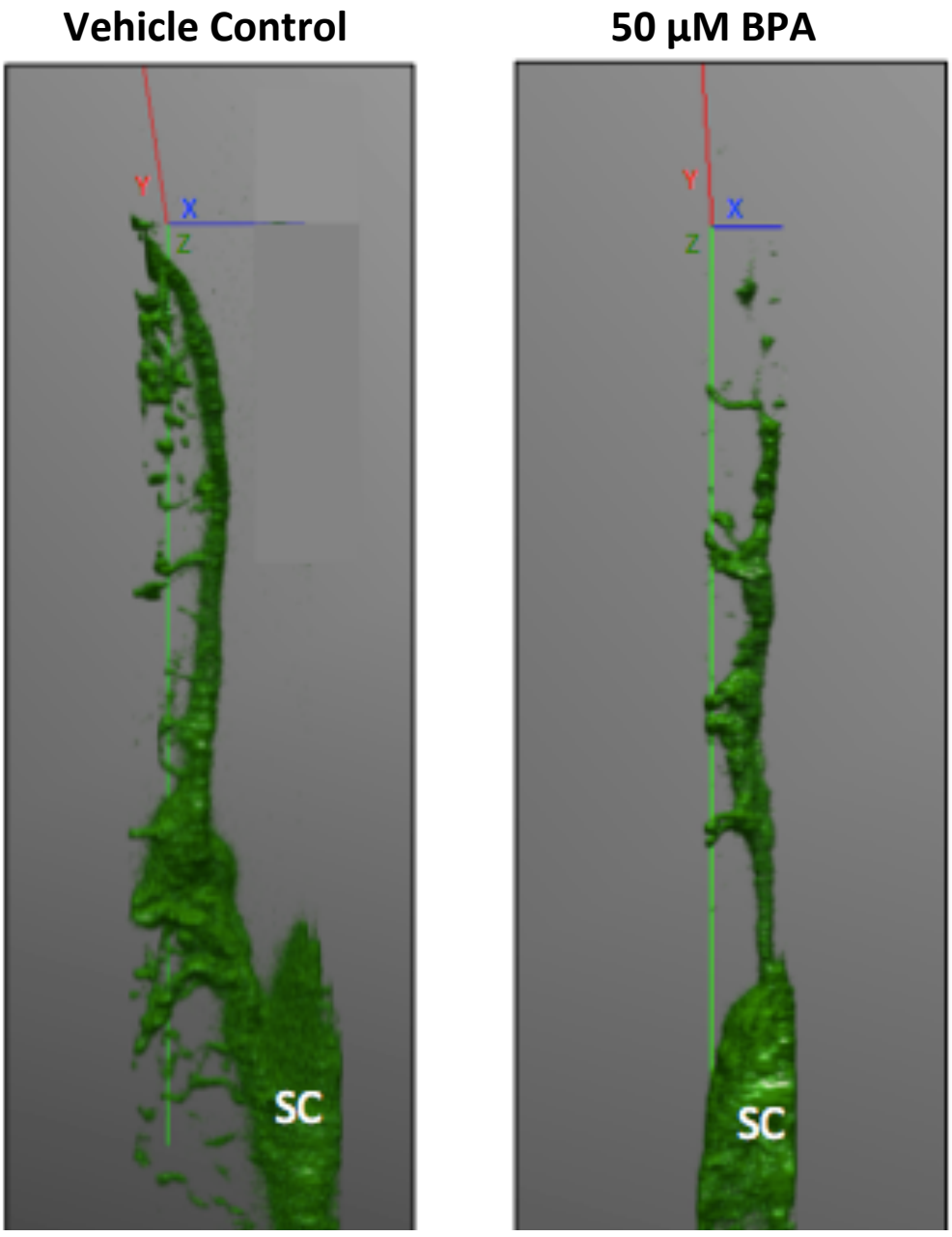

Figure 4.2 Defective Motor Axons Have a Normal Trajectory From the Spinal Cord. ***Tg:mnx1-GFP*** **embryos exposed to BPA have a similar axonal trajectory through the Z axis (green) as vehicle controls.**

4.3.2 Motor Neuron Cell Death

Colocalization between GFP+/ PI+ cells in the spinal cord within the 6 - 10 somite region shows evidence that 50 μM BPA exposed embryos have significantly increased motor cell death as evidenced by PI+/GFP+ cells at 72 hpf and 96 hpf (Figure 4.3; P = 0.006 and P = 0.008, respectively, Mann-Whitney U test) as compared to vehicle controls. This is suggestive that reduced motor axon length resulting from BPA exposure is associated motor neuron cell death. Data are based on the mean value of N = 7 - 12 biological replicates ±SD. Together, these results provide evidence that using motor axon length is a valid marker of motor neuron degeneration in BPA-exposed embryos.

Table 4.1 Duration of BPA Exposure on Mortality

	24 hpf	**48 hpf**	**72 hpf**	**96 hpf**	**120 hpf**
Vehicle Control	3.9%	0%	1.6%	0%	0%
50 μM BPA	1.9%	2.0%	5.7%	40%	100%

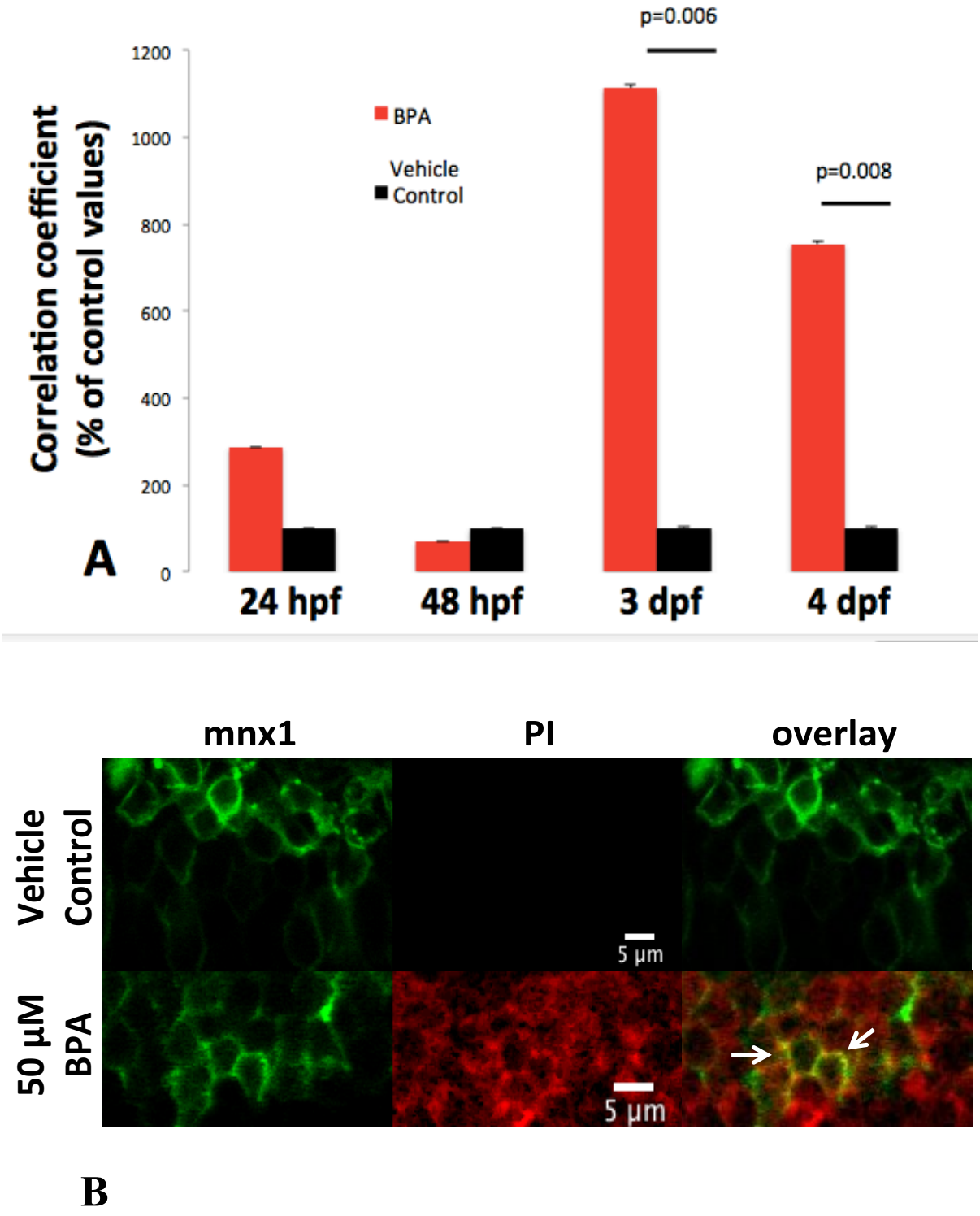

Figure 4.3 BPA Exposure Causes Increased Motor Cell Death. A) Motor neuron cell death is increased starting at 72 hpf following BPA exposure as evidence by PI+ motor neuron soma in the spinal cord (biological N = 7 – 12). Values indicate correlation coefficients as a percent of control values. B) BPA-exposed embryos show increased PI+ cells at 72 hpf as seen in the overlay image of mnx+/PI+ dead motor neuron cells, as indicated by the white arrows.

Chapter 5: Validating BPA as a sALS Model

5.1 Sporadic Models of ALS

Although fALS and sALS patients are clinically indistinguishable (14, 49), it's currently unknown whether both forms follow a similar disease pathogenesis (15). The majority of what we currently understand about the pathogenic mechanisms driving motor neuron degeneration is based on genetic models of the disease. Further, most investigative and therapeutic research has been based on models with mutations that lead to misfolded superoxide dismutase 1 (mSOD1) proteins, but these mutations only account for around 10% of fALS cases and less than 2% of all ALS patients (1, 13). Sporadic models should remain a priority for investigative and therapeutic research, although validated and effective animal models of sALS are currently lacking (19). Here, we investigated features of ALS hallmarks in order to determine if BPA-induced motor neuron toxicity in the zebrafish embryo is a valid sALS model.

5.2 Materials and methods

5.2.1 Zebrafish Lines

We use the wild type AB and the transgenic lines *Tg:mnx1-GFP* and *Tg:pU1::Gal4-UAS::TagRFP* (33) zebrafish strains for all experiments listed in Chapter 5. Zebrafish maintenance and husbandry is described in section 2.1.1. The transgenic *Tg:pU1::Gal4-UAS::TagRFP* strain was RFP expression driven by the pU1 promoter, labeling cells of myeloid lineage. Double transgenic embryos were created by cross breeding *Tg:mnx1-GFP* x *Tg:pU1::Gal4-UAS::TagRFP* and screening for transgene reporter heterozygocity (GFP+/RFP+ embryos) at 24 hpf using the fluorescence microscope

5.2.2 Neuromuscular Junction (NMJ) Labeling

Embryos treated with vehicle control or 50 μM BPA were fixed as described above and permeablized using 10 μg/ml proteinase K solution. Proteinase K solution was prepared by dissolving 200 μg /ml proteinase K in 50 mM Tris HCl pH 9 and 5mM $CaCl_2$. Whole mount immunohistochemistry was performed using znp-1 (or anti-synaptotagmin 2) primary antibody to label pre-synaptic motor axon terminals as described in section 2.2.6 with the following slight modification: prior to goat anti-mouse FITC 2^0Ab incubation, embryos were incubated in 10 μg/ml α-Bungarotoxin for 30 min at room temperature. Embryos were then washed with PBS-TS (1 X 30min) before the 2^0Ab was applied.

5.2.3 Analysis of NMJ Integrity

Embryos were flat mounted as described in section 2.2.7 and imaged by confocal microscopy using a 20x objective as detailed in 2.2.8. Analysis of the NMJ was performed using the Coloc2 plugin in the FIJI (a version of ImageJ) software. Z-stack lsm files were uploaded to the software and the channels were split. The background was subtracted for each stack in both channels with a rolling ball radius of 50 pixels and a region of interest was selected to encompass the motor axons and branches (spinal cord excluded). Colocalization analysis between synaptotagmin 2 and α-Bungarotoxin was performed for each Z-stack and Costes threshold was applied. Pearson's R^2 correlation coefficient was used to quantify colocalization. The colocalization between pre- and post-synaptic terminals of 5 axons per embryo (5 technical replicates) was recorded.

5.2.4 Microglia Phenotype

Microglia phenotype was determined based on morphology of RFP-labeled pU1+ cells in the spinal cord and surrounding motor axons. At 6 hpf, *Tg:mnx1-GFP/pU1-RFP* double transgenic embryos were subjected to chronic, non-static exposure to either 50 μM BPA or vehicle control and fixed at 48 hpf in 4% PFA as described in section 2.2.5. The region of interest was determined to be motor neuron soma in the spinal cord and the ventrally projecting motor axons. pU1+ microglial cells spatially associated with the region of interest were imaged whole mount by confocal microscopy. Z-stack files from the sagittal plane of the spinal cord region within the 6 - 10 somite region were collected using a 20x objective lens under a Zeiss LSM 510 confocal microscope. Z-stack files were reconstructed into maximum projection images and the morphology of microglia was graded based on previously published criteria (50). A pU1+ cell was graded if its complete structure was included in the region of interest. Morphology was graded on a spectrum of characteristic morphologies indicative of activated to resting microglia: amoeboid, stout processes, thick long processes, or thin ramified processes (see Figure 5.2). The proportion of microglia in each morphology was reported as a marker of activation state in each treatment group.

5.3 Results

Results show that BPA exposure induces an ALS-like phenotype, as evidenced by impaired motor function, reduced neuromuscular junction (NMJ) integrity, and evidence of microglial activation.

5.3.1 Effect of BPA on Motor Behaviour

The motor behaviour following BPA exposure was investigated to determine if motor axon abnormalities result in impaired motor function. Wild type embryos were exposed to 50 µM BPA, control or vehicle control and motor function was determined using TEER at 24 hpf and 48 hpf. BPA exposed embryos had 86.7% and 100% impaired motor function at 24 hpf and 48 hpf, respectively (Table 5.1, N = 15 biological replicates).

Table 5.1. BPA Exposure Affects Motor Function. Wild type embryos treated with 50 µM BPA show affected motor behaviour as indicated by touch evoked escape response (TEER) at 24 hpf and 48 hpf compared to control and vehicle control embryos (biological N = 15).

	Control	Vehicle Control	50 µM BPA
24 hpf	6.7%	0%	86.7%
48 hpf	0%	0%	100%

5.4 Neuromuscular Junction (NMJ) Integrity Following Exposure to BPA

The NMJ integrity was analyzed to support results of the abnormal motor axon phenotype and affected motor behaviour. Pearson's R^2 colocalization values between pre-synaptic (synaptotagmin 2) and post-synaptic (α-Bungarotoxin) terminals show that embryos exposed to 50 µM BPA have significantly reduced NMJ integrity at 48 hpf as compared to vehicle controls ($P = 0.006$, Mann-Whitney U test) and controls ($P = 0.02$; Mann-Whitney U test). Data are based on the mean value of N = 8 - 15 biological replicates.

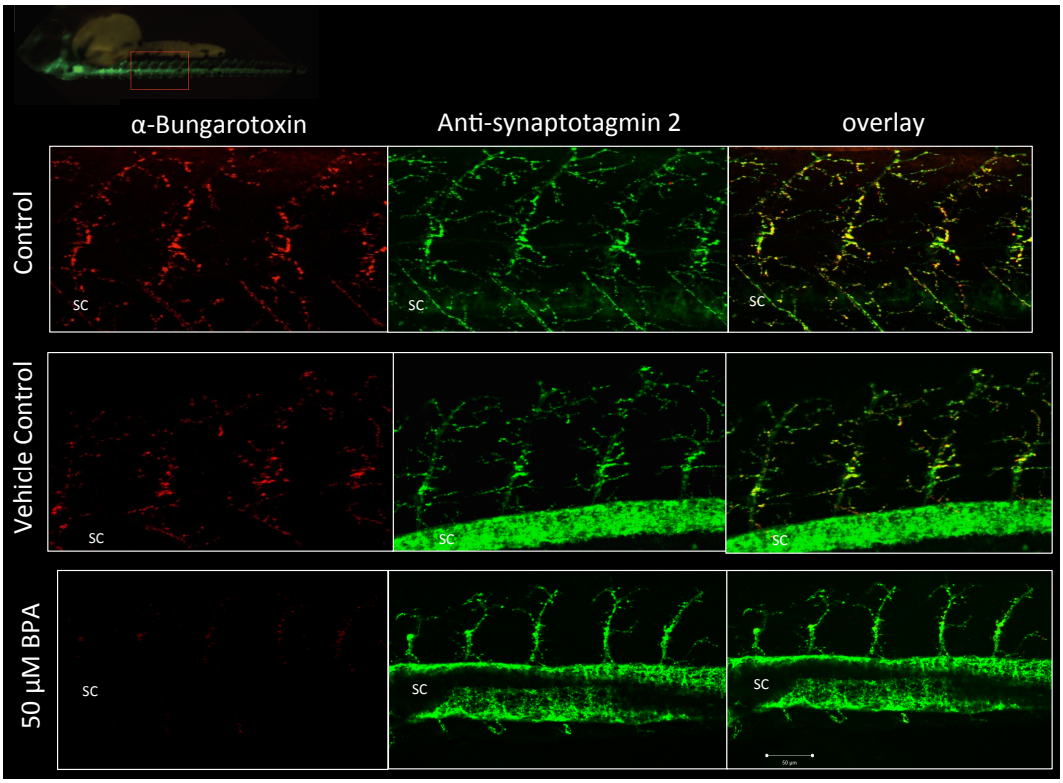

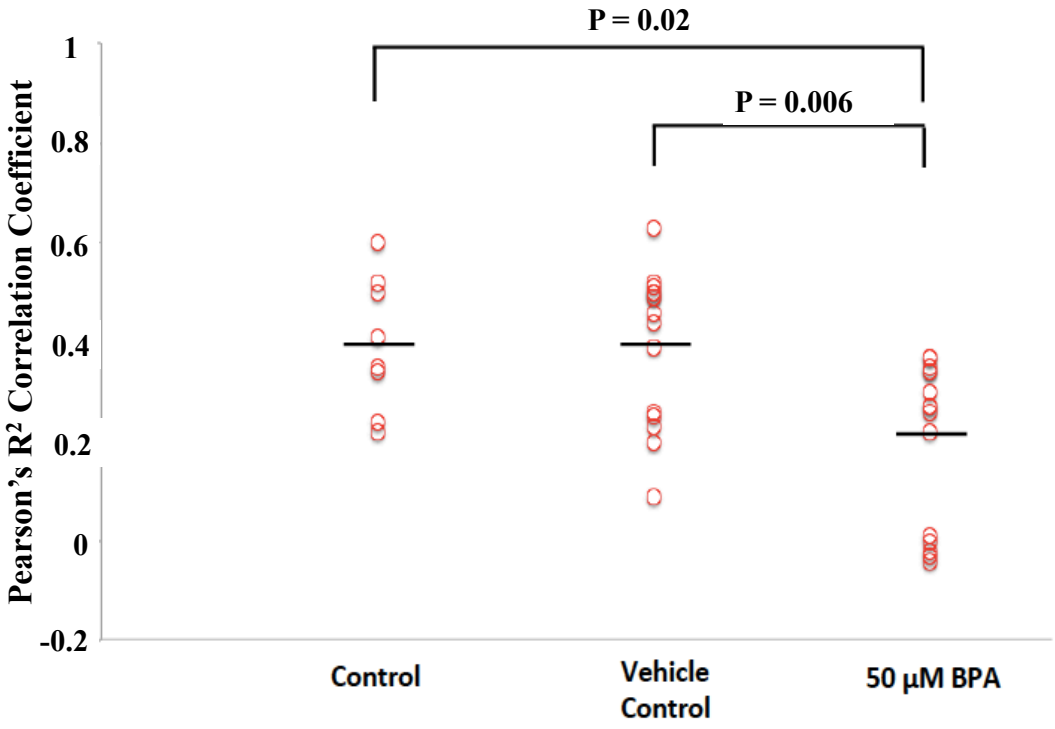

Figure 5.1 BPA Exposure Impairs NMJ Integrity. Embryos exposed to BPA have significantly reduced colocalization between pre- and post-synaptic terminals as compared to both controls (P = 0.02; N = 8-15) and vehicle controls (P = 0.006; N = 15); SC = spinal cord.

5.5 Microglia activation following BPA exposure

RFP-labeled pU1+ microglia cells spatially associated with abnormal motor axons and the spinal cord were graded based on the morphology indicative of activation state. Results show that embryos exposed to 50 µM BPA have a higher proportion of microglia in an activated state: 40% amoeboid microglia, 0% microglia with thin ramified processes (Figure 5.2, N = 9 biological replicates) compared to vehicle controls: 1% amoeboid microglia, 16% microglia with thin ramified processes (N = 12 biological replicates).

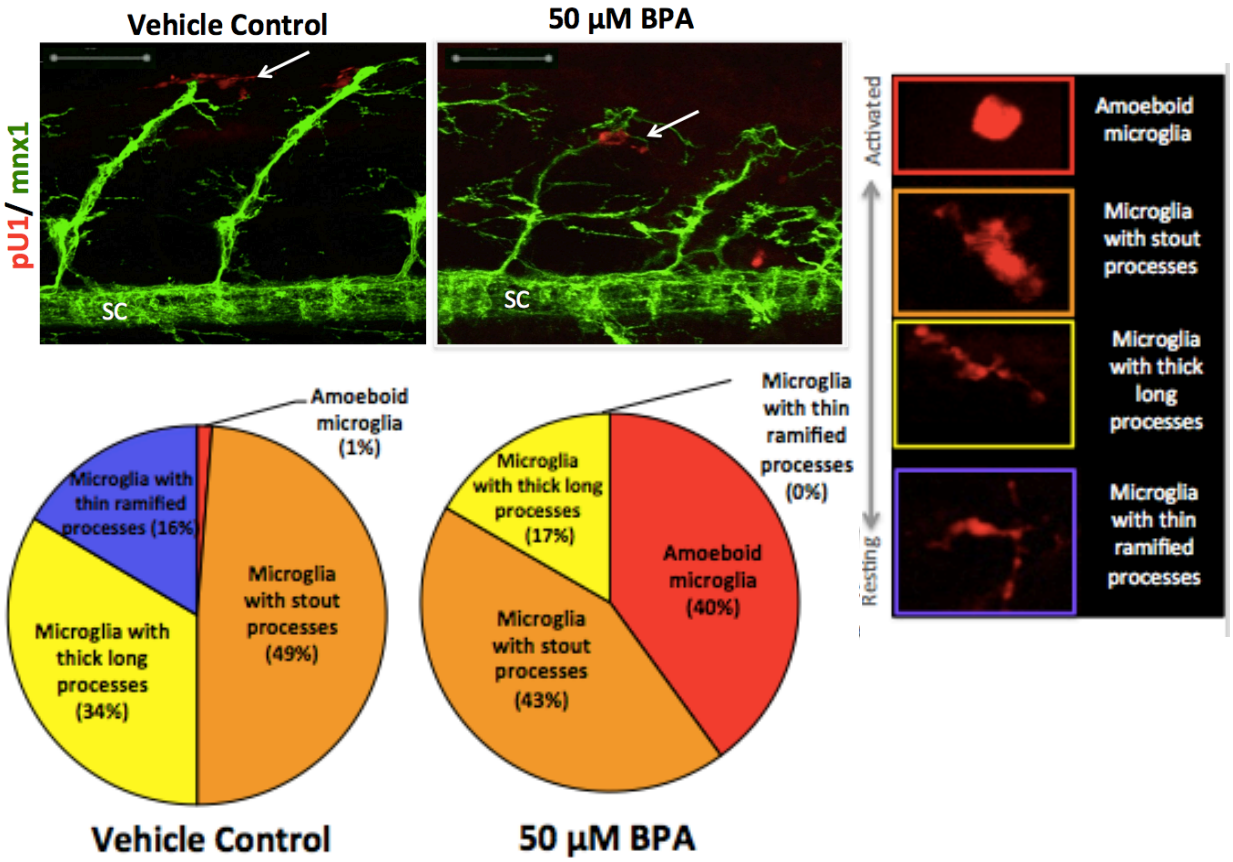

Figure 5.2. Activated Microglia Associate With Defective Motor Neurons. Double transgenic *Tg:mnx1-GFP/pU1-RFP* embryos exposed to BPA show that microglia spatially associated with defective motor neurons are in a more activated morphology. White arrows point to pu1+ microglial cells spatially associated with motor neurons. N = 9-12; SC = spinal cord; Scale bar = 50µm.

Chapter 6: Conclusion

6.1 Neurotoxin Exposure Induces an ALS-like Phenotype in Zebrafish Embryos

Results from this project provide evidence that zebrafish are efficient for screening motor neuron death induced by neurotoxins and are useful for modeling sALS. This can be used in future studies as an effective method to screen neurotoxins that have been linked to ALS through epidemiological studies in order to further investigate this relationship and pathogenesis. An important limitation of this study is that it is based on modeling adult-onset neurodegeneration in a developing embryo.

6.1.1 Neuromuscular Junction Degeneration in ALS

A characteristic feature of ALS patients in degeneration of the NMJ (51). Two different hypothesis of motor neuron dysfunction have been proposed: anterograde degeneration, where dysfunction initiates in the upper motor neurons and progresses to lower motor neurons, and retrograde degeneration, where dysfunction begins at the NMJ level and progresses to the motor axon soma (51). There is evidence for both anterograde (52) and retrograde (53) degeneration in ALS pathogenesis, however it is currently unknown where motor neuron dysfunction initiates or if both occur concurrently (51). Evidence from this project shows that integrity of the NMJ is impaired (Figure 5.1) and motor neurons have reduced motor axon length at 48 hpf (Figure 3.3), while evidence of motor cell death reaches significance starting at 72 hpf (Figure 4.3). These results suggest a retrograde mechanism of degeneration in toxin-induced neurotoxicity (Appendix B), where the motor axons first retract from the NMJ, then begin to undergo cell death. Further studies are warranted to more thoroughly investigate this degenerative process.

6.1.2 Microglia Activation in ALS

As the resident macrophages of the central nervous system, quiescent microglia function to monitor their direct surroundings by dynamic projections of their thin ramified processes to maintain homeostasis (54). In a non-disease state, glial cells surround motor neurons and provide them with neurotrophic support (55, 56). When microglia detect imbalances such as pathologic stimuli, they become activated and retract their processes to adopt a stereotypical amoeboid morphology (54). Activated microglia were traditionally believed to exist as either anti- or pro-inflammatory, neither of which are morphologically distinct (54). However, it is now understood that microglia exist on an inflammatory spectrum and express both pro- and anti-inflammatory markers simultaneously (54, 57). A more accurate characterization of activated microglia involves the evaluation of their specific inflammatory repertoire (57), nomenclature which has yet to be developed.

Microglia are now understood to have an operative role during ALS pathogenesis, where pronounced activation is evident in both patient tissue and *in vivo* models (58, 59). Microglia during early disease pathogenesis exist in a neurotrophic state and are associated with a more anti-inflammatory profile which progresses to a pro-inflammatory, neurotoxic state during later disease stages (60). However, the microglial phenotype is directly affected by their direct microenvironment and removing microglia from their native milieu can skew the phenotype, questioning the relevance on microglia *in vitro* studies (54). Here, we show find evidence of microglia activation from environmental stressor-induced motor neuron toxicity in an *in vivo* model (Figure 5.2), which supports BPA-induced neurotoxicity as a valid model of sALS. The

specific inflammatory phenotype and role that microglia have in toxin-induced motor neuron degeneration requires further analysis.

6.2 BPA as a Xenoestrogen

BPA is an industrial plasticizer which humans are ubiquitously exposed to through various routes, such as plastic bottles and dental sealants (61). BPA has been well characterized as an endocrine disruptor, including its role as a potential carcinogen (62-64). It is known to either activate or antagonize many different receptors such as estrogen receptors (ERs) α and β (65), membrane-bound estrogen receptor GPR30, glucocorticoid receptors and androgen receptors (AR) (61).

BPA is structurally similar to 17β-Estradiol (E2), the most prevalent estrogen in humans. As a xenoestrogen, BPA is known to bind to ERs and elicit weak estrogenic properties (61, 63, 66). It has been established that E2 has a neuroprotective effect on in spinal motor neurons (67, 68) and has been proposed as a potential therapeutic for ALS patients (69, 70). The mechanism of neuroprotection is believed to function independently of ER-mediated mechanisms (67, 68), and it is currently unclear whether antioxidant activity (67, 68) or the GPR30 (67, 71) is promoting cell survival. Further, there is evidence that estradiol protects motor neurons via the phosphatidylinositol 3-kinase/protein kinase B (PI3K/Akt) pathway (71). The PI3K/Akt pathway offers neuroprotection through anti-apoptotic effects and supports cell proliferation (63, 66, 71, 72).

6.2.1 The Effect of BPA on Neurotoxicity

A number of studies have shown evidence that BPA exposure results in altered motor effects (46, 73, 74). BPA alters the quantity of neurotransmitters such as acetyl cholinesterase and has been linked to neurodegeneration (75). Zebrafish embryos exposed to BPA show adverse affects on motor axon length, musculature and motor behaviour along with evidence of increased cell death (46). There is also evidence that BPA drives motor neuron toxicity in rodent models (61, 71), perhaps by hydroxyl radical formation (75) or through non-androgenic receptor pathways (61). However, the mechanism driving motor dysfunction and toxicity induced by BPA is not well understood to date.

As a xenoestrogen, it's currently unclear why BPA and E2 have opposing effects on motor neurons, although exposure dose may be a confounding factor. There is evidence that different exposure doses of BPA produce discordant effects on cell viability, where relatively low exposures (~2 μM) result in cell proliferation and increased viability and higher exposures (>100 μM) result in decreased cell proliferation and evidence of cell death (76). Since BPA is known to bind to many different receptors and there is evidence that E2 drives neuroprotection through ER-independent pathways, it is also possible that BPA and E2 drive motor effects through unique ER-independent mechanisms.

6.3 Motor Axon Length is Representative of Motor Neuron Degeneration

In this project, we have confirmed that motor axon length is a reliable surrogate marker of motor neuron degeneration. We provide evidence that the motor axon trajectory through the Z-axis is similar in both toxin-exposed and vehicle control embryos. This suggests that the axon length

from the 2-dimensional sagittal plane reliably represents the true 3-dimensional length. This is a novel in the current literature and confirms methodology from previous groups (39-42) who use this conventional sagittal view of the motor axon length in zebrafish embryos. Results from this project also confirm that reduced motor axon length is associated with increased motor cell death, confirming motor axon length as a surrogate marker of motor neuron degeneration. However, a more definitive mechanism of motor neuron degeneration requires further investigation. Together, these results support the validity of modeling sALS in a zebrafish through neurotoxin exposure.

6.4 Summary and Future Directions

Research based on modeling the genetic forms of ALS has failed to translate into any effective therapeutic interventions to date (77, 78). While it remains possible that modeling motor neuron degeneration using genetic mutations may provide meaningful insights into sALS pathogenesis, it is more likely that initial cellular dysfunctions are driven by different mechanisms. This may limit the use of fALS models in providing meaningful insights into the pathogenesis of 90% of patients. In this project, we have shown that zebrafish can be an efficient model for screening neurotoxicity induced by environmental toxins. We also provide evidence that quantifying motor axon length from the sagittal plane in defective motor axons is a valid marker of its length through the Z-axis. Further, we have shown that environmentally induced neurotoxicity elicited by BPA exposure recapitulates key hallmarks of ALS pathology in the zebrafish embryo. This provides evidence that BPA-induced neurotoxicity can be used as a valid model of sALS and more generally that neurotoxin-induced motor neuron degeneration in a zebrafish embryo may prove insightful into sALS pathogenesis. Future studies of sALS in zebrafish could be focused

on high throughput neurotoxin screening of motor neuron defects using epidemiologically relevant environmental stressors that have been implicated in sALS. These studies could be further extended to investigate the pathogenic mechanisms driving motor neuron death following neurotoxin exposure. The findings could be compared to studies investigating the pathogenesis of fALS in order to determine if motor neuron degeneration is being driven by a similar mechanism in each sALS and fALS models. This information is critical when evaluating if research based on fALS models can be extended to sALS.

References:

1. Turner MR, Swash M. The expanding syndrome of amyotrophic lateral sclerosis: a clinical and molecular odyssey. Journal of neurology, neurosurgery, and psychiatry. 2015;86(6):667-73.
2. Al-Chalabi A, Hardiman O. The epidemiology of ALS: a conspiracy of genes, environment and time. Nature reviews Neurology. 2013;9(11):617-28.
3. Salameh JS, Brown RH, Jr., Berry JD. Amyotrophic Lateral Sclerosis: Review. Seminars in neurology. 2015;35(4):469-76.
4. Swinnen B, Robberecht W. The phenotypic variability of amyotrophic lateral sclerosis. Nature reviews Neurology. 2014;10(11):661-70.
5. Ajroud-Driss S, Siddique T. Sporadic and hereditary amyotrophic lateral sclerosis (ALS). Biochimica et Biophysica Acta (BBA) - Molecular Basis of Disease. 2015;1852(4):679-84.
6. Clerc P, Lipnick S, Willett C. A look into the future of ALS research. Drug Discovery Today.
7. Bellingham MC. A review of the neural mechanisms of action and clinical efficiency of riluzole in treating amyotrophic lateral sclerosis: what have we learned in the last decade? CNS neuroscience & therapeutics. 2011;17(1):4-31.
8. (FDA) USFaDA. FDA approves drug to treat ALS. In: (FDA) USFaDA, editor. May 5, 2017.
9. Canada A. A second ALS treatment, edaravone, has been newly approved in the United States. https://www.als.ca/blogs/second-als-treatment-edaravone-newly-approved-united-states/ May 8 2017 [
10. Haeusler AR, Donnelly CJ, Periz G, Simko EA, Shaw PG, Kim MS, et al. C9orf72 nucleotide repeat structures initiate molecular cascades of disease. Nature. 2014;507(7491):195-200.
11. Marangi G, Traynor BJ. Genetic causes of amyotrophic lateral sclerosis: New genetic analysis methodologies entailing new opportunities and challenges. Brain research. 2015;1607:75-93.
12. Renton AE, Majounie E, Waite A, Simon-Sanchez J, Rollinson S, Gibbs JR, et al. A hexanucleotide repeat expansion in C9ORF72 is the cause of chromosome 9p21-linked ALS-FTD. Neuron. 2011;72(2):257-68.
13. Haulcomb MM, Mesnard NA, Batka RJ, Alexander TD, Sanders VM, Jones KJ. Axotomy-induced target disconnection promotes an additional death mechanism involved in motoneuron degeneration in amyotrophic lateral sclerosis transgenic mice. The Journal of comparative neurology. 2014;522(10):2349-76.
14. Gros-Louis F, Gaspar C, Rouleau GA. Genetics of familial and sporadic amyotrophic lateral sclerosis. Biochimica et Biophysica Acta (BBA) - Molecular Basis of Disease. 2006;1762(11–12):956-72.
15. Laferriere F, Polymenidou M. Advances and challenges in understanding the multifaceted pathogenesis of amyotrophic lateral sclerosis. Swiss medical weekly. 2015;145:w14054.
16. Mostafalou S, Abdollahi M. Pesticides: an update of human exposure and toxicity. Archives of toxicology. 2017;91(2):549-99.
17. Oskarsson B, Horton DK, Mitsumoto H. Potential Environmental Factors in Amyotrophic Lateral Sclerosis. Neurologic clinics. 2015;33(4):877-88.

18. Bozzoni V, Pansarasa O, Diamanti L, Nosari G, Cereda C, Ceroni M. Amyotrophic lateral sclerosis and environmental factors. Functional neurology. 2016;31(1):7-19.
19. Merwin SJ, Obis T, Nunez Y, Re DB. Organophosphate neurotoxicity to the voluntary motor system on the trail of environment-caused amyotrophic lateral sclerosis: the known, the misknown, and the unknown. Archives of toxicology. 2017:1-14.
20. Plato CC, Garruto RM, Fox KM, Gajdusek DC. Amyotrophic lateral sclerosis and parkinsonism-dementia on Guam: a 25-year prospective case-control study. American journal of epidemiology. 1986;124(4):643-56.
21. Arnold A, Edgren DC, Palladino VS. Amyotrophic lateral sclerosis; fifty cases observed on Guam. The Journal of nervous and mental disease. 1953;117(2):135-9.
22. Reed DM, Brody JA. Amyotrophic lateral sclerosis and parkinsonism-dementia on Guam, 1945-1972. I. Descriptive epidemiology. American journal of epidemiology. 1975;101(4):287-301.
23. Yase Y, Yoshida S, Kihira T, Wakayama I, Komoto J. Kii ALS dementia. Neuropathology : official journal of the Japanese Society of Neuropathology. 2001;21(2):105-9.
24. Beard JD, Kamel F. Military service, deployments, and exposures in relation to amyotrophic lateral sclerosis etiology and survival. Epidemiologic reviews. 2015;37:55-70.
25. Beghi E. Are professional soccer players at higher risk for ALS? Amyotrophic lateral sclerosis & frontotemporal degeneration. 2013;14(7-8):501-6.
26. Abel EL. Football increases the risk for Lou Gehrig's disease, amyotrophic lateral sclerosis. Perceptual and motor skills. 2007;104(3 Pt 2):1251-4.
27. Kamel F, Umbach DM, Bedlack RS, Richards M, Watson M, Alavanja MC, et al. Pesticide exposure and amyotrophic lateral sclerosis. Neurotoxicology. 2012;33(3):457-62.
28. Merwin SJ, Obis T, Nunez Y, Re DB. Organophosphate neurotoxicity to the voluntary motor system on the trail of environment-caused amyotrophic lateral sclerosis: the known, the misknown, and the unknown. Archives of toxicology. 2017.
29. Wilson JM, Khabazian I, Wong MC, Seyedalikhani A, Bains JS, Pasqualotto BA, et al. Behavioral and neurological correlates of ALS-parkinsonism dementia complex in adult mice fed washed cycad flour. Neuromolecular medicine. 2002;1(3):207-21.
30. Babin PJ, Goizet C, Raldua D. Zebrafish models of human motor neuron diseases: advantages and limitations. Progress in neurobiology. 2014;118:36-58.
31. Goessling W, North TE, Zon LI. New Waves of Discovery: Modeling Cancer in Zebrafish. Journal of Clinical Oncology. 2007;25(17):2473-9.
32. Ali S, Champagne DL, Spaink HP, Richardson MK. Zebrafish embryos and larvae: a new generation of disease models and drug screens. Birth defects research Part C, Embryo today : reviews. 2011;93(2):115-33.
33. Mazaheri F, Breus O, Durdu S, Haas P, Wittbrodt J, Gilmour D, et al. Distinct roles for BAI1 and TIM-4 in the engulfment of dying neurons by microglia. Nature communications. 2014;5:4046.
34. He J-H, Gao J-M, Huang C-J, Li C-Q. Zebrafish models for assessing developmental and reproductive toxicity. Neurotoxicology and Teratology. 2014;42:35-42.
35. Sassen W, Köster R. A molecular toolbox for genetic manipulation of zebrafish. Advances in Genomics and Genetics. 2015;2015(1):151-63.
36. Myers PZ. Spinal motoneurons of the larval zebrafish. The Journal of comparative neurology. 1985;236(4):555-61.

37. Westerfield M, McMurray JV, Eisen JS. Identified motoneurons and their innervation of axial muscles in the zebrafish. The Journal of neuroscience : the official journal of the Society for Neuroscience. 1986;6(8):2267-77.
38. Rodino-Klapac LR, Beattie CE. Zebrafish topped is required for ventral motor axon guidance. Developmental Biology. 2004;273(2):308-20.
39. Ciura S, Lattante S, Le Ber I, Latouche M, Tostivint H, Brice A, et al. Loss of function of C9orf72 causes motor deficits in a zebrafish model of amyotrophic lateral sclerosis. Annals of neurology. 2013;74(2):180-7.
40. Kabashi E, Bercier V, Lissouba A, Liao M, Brustein E, Rouleau GA, et al. FUS and TARDBP but not SOD1 interact in genetic models of amyotrophic lateral sclerosis. PLoS genetics. 2011;7(8):e1002214.
41. Schmid B, Hruscha A, Hogl S, Banzhaf-Strathmann J, Strecker K, van der Zee J, et al. Loss of ALS-associated TDP-43 in zebrafish causes muscle degeneration, vascular dysfunction, and reduced motor neuron axon outgrowth. Proceedings of the National Academy of Sciences of the United States of America. 2013;110(13):4986-91.
42. Lattante S, de Calbiac H, Le Ber I, Brice A, Ciura S, Kabashi E. Sqstm1 knock-down causes a locomotor phenotype ameliorated by rapamycin in a zebrafish model of ALS/FTLD. Human molecular genetics. 2015;24(6):1682-90.
43. Westerfield M. The zebrafish book: a guide for the laboratory use of zebrafish (Brachydanio rerio): University of Oregon press; 1995.
44. Kanungo J, Cuevas E, Ali SF, Paule MG. Ketamine induces motor neuron toxicity and alters neurogenic and proneural gene expression in zebrafish. Journal of applied toxicology : JAT. 2013;33(6):410-7.
45. Senger MR, Seibt KJ, Ghisleni GC, Dias RD, Bogo MR, Bonan CD. Aluminum exposure alters behavioral parameters and increases acetylcholinesterase activity in zebrafish (Danio rerio) brain. Cell biology and toxicology. 2011;27(3):199-205.
46. Wang X, Dong Q, Chen Y, Jiang H, Xiao Q, Wang Y, et al. Bisphenol A affects axonal growth, musculature and motor behavior in developing zebrafish. Aquatic toxicology (Amsterdam, Netherlands). 2013;142-143:104-13.
47. University C. Dose-Response Relationships In Toxicology Toxicology Information Briefs [Internet]. 1993.
48. Flanagan-Steet H, Fox MA, Meyer D, Sanes JR. Neuromuscular synapses can form in vivo by incorporation of initially aneural postsynaptic specializations. Development (Cambridge, England). 2005;132(20):4471-81.
49. Haidet-Phillips AM, Hester ME, Miranda CJ, Meyer K, Braun L, Frakes A, et al. Astrocytes from Familial and Sporadic ALS Patients are Toxic to Motor Neurons. Nature biotechnology. 2011;29(9):824-8.
50. Schwarz JM, Sholar PW, Bilbo SD. Sex differences in microglial colonization of the developing rat brain. Journal of neurochemistry. 2012;120(6):948-63.
51. Campanari ML, Garcia-Ayllon MS, Ciura S, Saez-Valero J, Kabashi E. Neuromuscular Junction Impairment in Amyotrophic Lateral Sclerosis: Reassessing the Role of Acetylcholinesterase. Frontiers in molecular neuroscience. 2016;9:160.
52. Casas C, Herrando-Grabulosa M, Manzano R, Mancuso R, Osta R, Navarro X. Early presymptomatic cholinergic dysfunction in a murine model of amyotrophic lateral sclerosis. Brain and behavior. 2013;3(2):145-58.

53. Fischer LR, Culver DG, Tennant P, Davis AA, Wang M, Castellano-Sanchez A, et al. Amyotrophic lateral sclerosis is a distal axonopathy: evidence in mice and man. Experimental neurology. 2004;185(2):232-40.
54. Cartier N, Lewis CA, Zhang R, Rossi FM. The role of microglia in human disease: therapeutic tool or target? Acta neuropathologica. 2014;128(3):363-80.
55. Philips T, Rothstein JD. Glial cells in amyotrophic lateral sclerosis. Experimental neurology. 2014;262 Pt B:111-20.
56. Turnquist C, Horikawa I, Foran E, Major EO, Vojtesek B, Lane DP, et al. p53 isoforms regulate astrocyte-mediated neuroprotection and neurodegeneration. Cell death and differentiation. 2016;23(9):1515-28.
57. Cherry JD, Olschowka JA, O'Banion MK. Neuroinflammation and M2 microglia: the good, the bad, and the inflamed. Journal of neuroinflammation. 2014;11:98.
58. Hall ED, Oostveen JA, Gurney ME. Relationship of microglial and astrocytic activation to disease onset and progression in a transgenic model of familial ALS. Glia. 1998;23(3):249-56.
59. McGeer PL, McGeer EG. Inflammatory processes in amyotrophic lateral sclerosis. Muscle & nerve. 2002;26(4):459-70.
60. Tang Y, Le W. Differential Roles of M1 and M2 Microglia in Neurodegenerative Diseases. Molecular neurobiology. 2016;53(2):1181-94.
61. Jones BA, Wagner LS, Watson NV. The Effects of Bisphenol A Exposure at Different Developmental Time Points in an Androgen-Sensitive Neuromuscular System in Male Rats. Endocrinology. 2016;157(8):2972-7.
62. Seachrist DD, Bonk KW, Ho SM, Prins GS, Soto AM, Keri RA. A review of the carcinogenic potential of bisphenol A. Reproductive toxicology (Elmsford, NY). 2016;59:167-82.
63. Ptak A, Wrobel A, Gregoraszczuk EL. Effect of bisphenol-A on the expression of selected genes involved in cell cycle and apoptosis in the OVCAR-3 cell line. Toxicology letters. 2011;202(1):30-5.
64. Mesnage R, Phedonos A, Arno M, Balu S, Christopher Corton J, Antoniou MN. Transcriptome profiling reveals bisphenol A alternatives activate estrogen receptor alpha in human breast cancer cells. Toxicological sciences : an official journal of the Society of Toxicology. 2017.
65. Sone K, Hinago M, Kitayama A, Morokuma J, Ueno N, Watanabe H, et al. Effects of 17beta-estradiol, nonylphenol, and bisphenol-A on developing Xenopus laevis embryos. General and comparative endocrinology. 2004;138(3):228-36.
66. Sengupta S, Obiorah I, Maximov PY, Curpan R, Jordan VC. Molecular mechanism of action of bisphenol and bisphenol A mediated by oestrogen receptor alpha in growth and apoptosis of breast cancer cells. British journal of pharmacology. 2013;169(1):167-78.
67. Nakamizo T, Urushitani M, Inoue R, Shinohara A, Sawada H, Honda K, et al. Protection of cultured spinal motor neurons by estradiol. Neuroreport. 2000;11(16):3493-7.
68. Culmsee C, Vedder H, Ravati A, Junker V, Otto D, Ahlemeyer B, et al. Neuroprotection by estrogens in a mouse model of focal cerebral ischemia and in cultured neurons: evidence for a receptor-independent antioxidative mechanism. Journal of cerebral blood flow and metabolism : official journal of the International Society of Cerebral Blood Flow and Metabolism. 1999;19(11):1263-9.

69. Blasco H, Guennoc A-M, Veyrat-Durebex C, Gordon PH, Andres CR, Camu W, et al. Amyotrophic lateral sclerosis: A hormonal condition? Amyotrophic Lateral Sclerosis. 2012;13(6):585-8.
70. Dykens JA, Moos WH, Howell N. Development of 17alpha-estradiol as a neuroprotective therapeutic agent: rationale and results from a phase I clinical study. Annals of the New York Academy of Sciences. 2005;1052:116-35.
71. Chen J, Hu R, Ge H, Duanmu W, Li Y, Xue X, et al. G-protein-coupled receptor 30-mediated antiapoptotic effect of estrogen on spinal motor neurons following injury and its underlying mechanisms. Molecular medicine reports. 2015;12(2):1733-40.
72. Ptak A, Rak-Mardyla A, Gregoraszczuk EL. Cooperation of bisphenol A and leptin in inhibition of caspase-3 expression and activity in OVCAR-3 ovarian cancer cells. Toxicology in vitro : an international journal published in association with BIBRA. 2013;27(6):1937-43.
73. Nojima K, Takata T, Masuno H. Prolonged exposure to a low-dose of bisphenol A increases spontaneous motor activity in adult male rats. The journal of physiological sciences : JPS. 2013;63(4):311-5.
74. Nagao T, Kawachi K, Kagawa N, Komada M. Neurobehavioral evaluation of mouse newborns exposed prenatally to low-dose bisphenol A. The Journal of toxicological sciences. 2014;39(2):231-5.
75. Masuo Y, Ishido M. Neurotoxicity of endocrine disruptors: possible involvement in brain development and neurodegeneration. Journal of toxicology and environmental health Part B, Critical reviews. 2011;14(5-7):346-69.
76. Tiwari SK, Agarwal S, Seth B, Yadav A, Ray RS, Mishra VN, et al. Inhibitory Effects of Bisphenol-A on Neural Stem Cells Proliferation and Differentiation in the Rat Brain Are Dependent on Wnt/beta-Catenin Pathway. Molecular neurobiology. 2015;52(3):1735-57.
77. Zwiegers P, Lee G, Shaw CA. Reduction in hSOD1 copy number significantly impacts ALS phenotype presentation in G37R (line 29) mice: implications for the assessment of putative therapeutic agents. Journal of negative results in biomedicine. 2014;13:14.
78. Turner BJ, Talbot K. Transgenics, toxicity and therapeutics in rodent models of mutant SOD1-mediated familial ALS. Progress in neurobiology. 2008;85(1):94-134.

Appendices

Appendix A

Table 6.1 Chemical Reagents

Chemical:	**Supplier:**
Ketamine HCl	Bioniche
Aluminum chloride ($AlCl_3$)	Sigma-Aldrich
Bisphenol A (BPA)	Sigma-Aldrich
Tween 20	Fisher Scientific
Triton X	BDH
Znp-1 monoclonal antibody	Developmental Studies Hybridoma Bank
FITC Goat anti-mouse secondary antibody	Jackson Laboratories
Vectashield fluorescence mounting media H-1000	Biolynx
Propidium Iodide	Sigma-Aldrich
PTU	Sigma-Aldrich
Normal Goat Serum	Vector Laboraties
α-Bungarotoxin (TRITC)	Life Technologies
Proteinase K	Promega
DMSO	Sigma-Aldrich
PFA	Sigma-Aldrich
DPX	Sigma-Aldrich
Tricaine	Sigma-Aldrich

Chemical:	**Supplier:**
Pronase	Roche
NaCl	Fisher Scientific
$CaCl_2$	Fisher Scientific
Methylene Blue	Fisher Scientific
KCl	Fisher Scientific
$MgCl_2$	BDH
Tris	Biorad
BSA	Sigma-Aldrich

Appendix B

Reduced Motor Axon Length At 48 Hpf Is Associated With Increased Motor Cell Death At 72 hpf. BPA-exposed embryos have reduced motor axon length at 48 hpf and increased motor cell death at 72 hpf compared to vehicle control, suggesting a "dying back" mechanism of motor neuron degeneration. Symbol represents the group mean, error bars represent SD, N = 9 – 10.

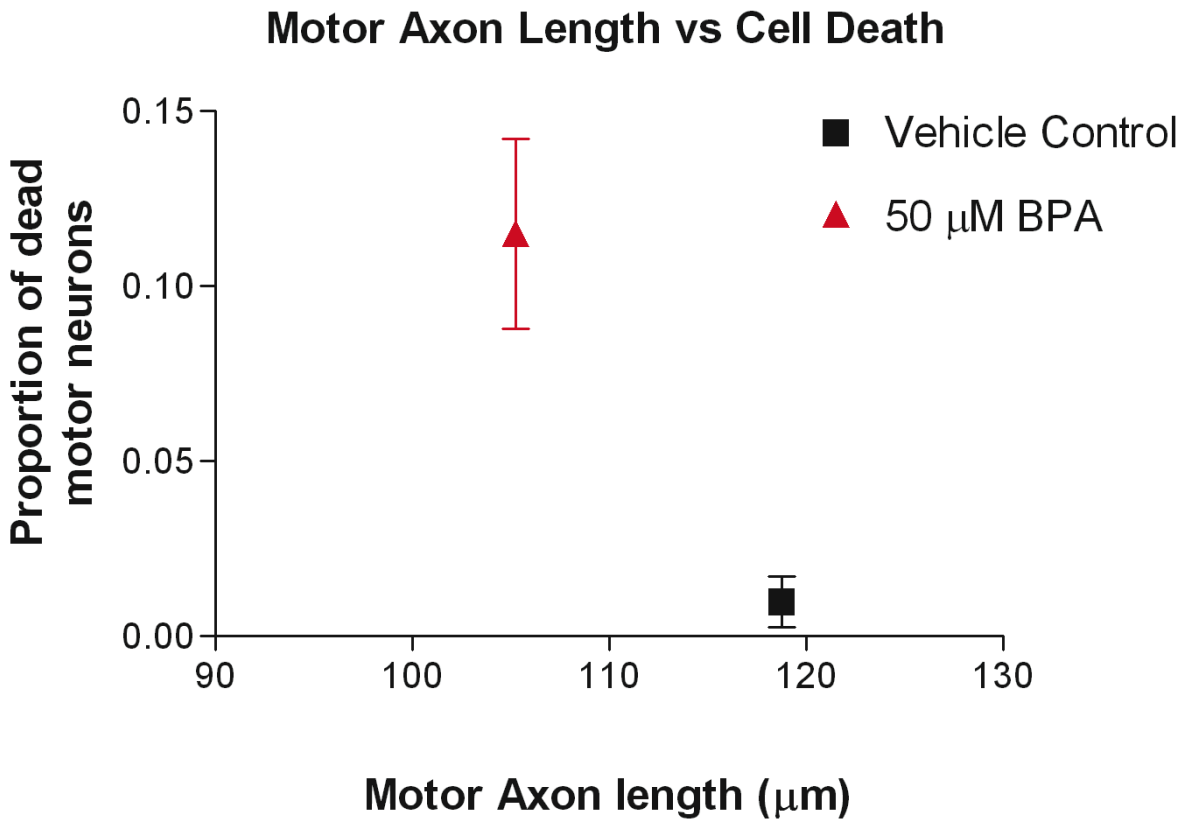

Appendix C

Teratogenic Effects of BPA. BPA-induced teratogenic effects at 24 hpf (A) and 48 hpf (B), such as cardiac edema, a bloated yolk sac extension and major morphological defects such as absence of tail. Embryos with major morphological defects were excluded from further analysis.

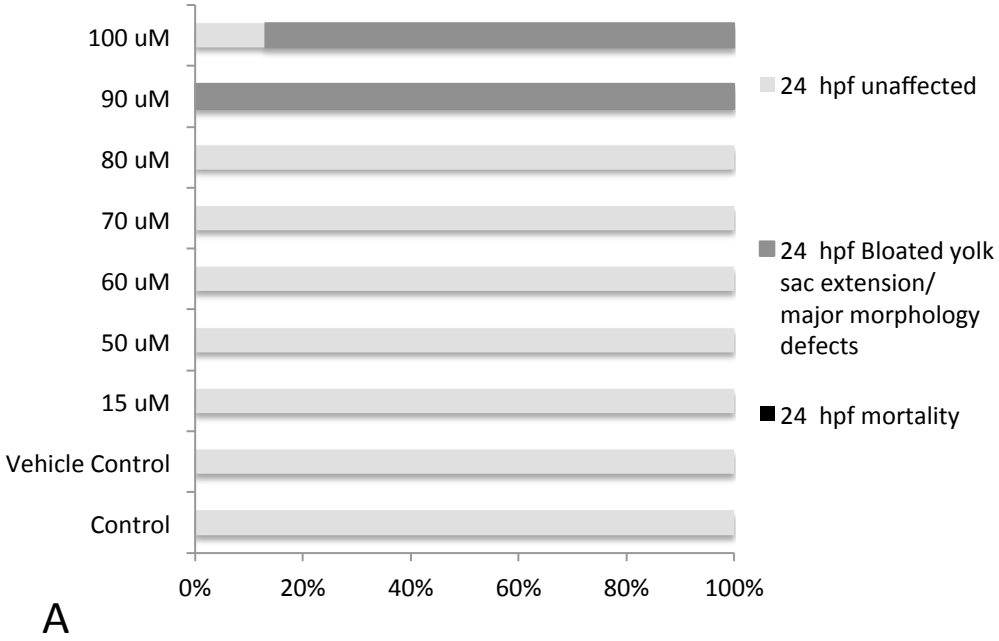

A

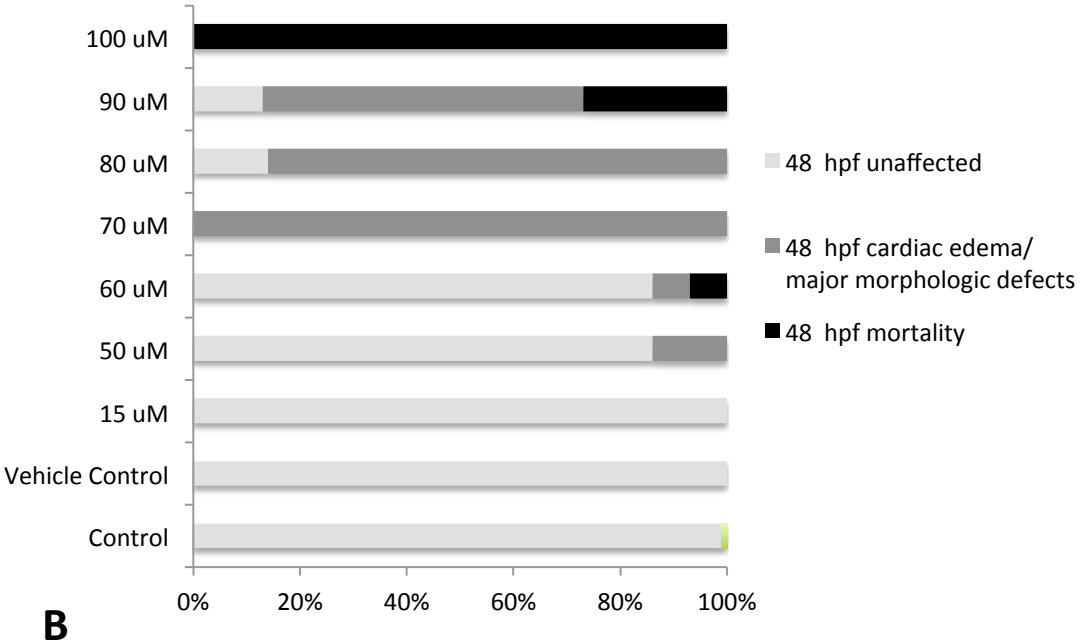

B

Appendix D

50 µM BPA Reduces Motor Axon Length. Motor axon length is significantly reduced at 50 µM BPA exposure compared to both control (P = 0.002; Kruskal-Wallis, Mann-Whitney U test) and vehicle control (P = 0.001; Mann-Whitney U test). Data are based on the mean of N = 5 – 6 technical replicates and N = 9 – 10 biological replicates.